





ARTICLE

Spatiotemporal restriction of endothelial cell calcium signaling is required during leukocyte transmigration

Prarthana J. Dalal¹, David P. Sullivan¹, Evan W. Weber¹, David B. Sacks², Matthias Gunzer³, Isabella M. Grumbach⁴, Joan Heller Brown⁵, and William A. Muller¹

Endothelial cell calcium flux is critical for leukocyte transendothelial migration (TEM), which in turn is essential for the inflammatory response. Intravital microscopy of endothelial cell calcium dynamics reveals that calcium increases locally and transiently around the transmigration pore during TEM. Endothelial calmodulin (CaM), a key calcium signaling protein, interacts with the IQ domain of IQGAP1, which is localized to endothelial junctions and is required for TEM. In the presence of calcium, CaM binds endothelial calcium/calmodulin kinase II δ (CaMKII δ). Disrupting the function of CaM or CaMKII with small-molecule inhibitors, expression of a CaMKII inhibitory peptide, or expression of dominant negative CaMKII δ significantly reduces TEM by interfering with the delivery of the lateral border recycling compartment (LBRC) to the site of TEM. Endothelial CaMKII is also required for TEM in vivo as shown in two independent mouse models. These findings highlight novel roles for endothelial CaM and CaMKII δ in transducing the spatiotemporally restricted calcium signaling required for TEM.

Introduction

In response to inflammatory stimuli, chemokines and cytokines released from damaged tissues activate the local endothelium to recruit circulating leukocytes. This process is crucial for resolving injury and eliminating infections but, when improperly regulated, can become the basis of many pathological conditions. Examples of such conditions include atherosclerosis, multiple sclerosis, and rheumatoid arthritis among many others. Thus, understanding the molecular mechanisms that govern leukocyte transendothelial migration (TEM) can help uncover novel therapeutic targets to ultimately reduce misdirected and unwanted inflammation (Muller, 2016a, 2016b).

Leukocyte recruitment involves a series of complex, adhesive interactions between circulating leukocytes and endothelial cells lining postcapillary venules. This ultimately culminates with leukocyte TEM or diapedesis, whereby leukocytes traverse the endothelial barrier to gain access to the damaged tissue. TEM is highly regulated and involves a number of sequential protein-protein interactions between leukocytes and endothelial cells that promote downstream endothelial signaling (Muller, 2011; Schenkel et al., 2002; Watson et al., 2015).

A transient increase in endothelial cytosolic free calcium concentration is also required to support TEM (Carman and Springer, 2004; Etienne-Manneville et al., 2000; Huang et al., 1993; Kielbassa-Schnepp et al., 2001; Su et al., 2000). Recent evidence has shown that transient receptor potential channel 6 (TRPC6) is the specific channel that mediates the calcium influx required for TEM (Dalal et al., 2020; Weber et al., 2015). Knockout and blockade of endothelial TRPC6 activity in vitro and in vivo both result in a profound defect in neutrophil TEM. However, relatively little is known regarding the spatiotemporal dynamics of the calcium influx during TEM and the implications this has for calcium-effector coupling.

Platelet endothelial cell adhesion molecule (PECAM), CD99, and other molecules involved in regulating TEM partially reside in a unique endothelial sub-junctional compartment called the lateral border recycling compartment (LBRC; Sullivan et al., 2013). During TEM, the LBRC moves to surround the trans-migrating leukocyte in a process called targeted recycling (Mamdouh et al., 2003). Directed movement of the LBRC during TEM provides additional membrane and unligated adhesion

¹Department of Pathology, Northwestern University Feinberg School of Medicine, Chicago, IL; ²Department of Laboratory Medicine, National Institutes of Health, Bethesda, MD; ³Institute for Experimental Immunology and Imaging, University Hospital, University Duisburg-Essen, Essen, Germany; ⁴Department of Internal Medicine, University of Iowa, Carver College of Medicine, Iowa City, IA; ⁵Department of Pharmacology, University of California, San Diego, La Jolla, CA.

Correspondence to William A. Muller: wamuller@northwestern.edu; E.W. Weber's present address is Stanford Cancer Institute, Stanford University School of Medicine, Stanford, CA.

© 2020 Dalal et al. This article is distributed under the terms of an Attribution–Noncommercial–Share Alike–No Mirror Sites license for the first six months after the publication date (see <http://www.rupress.org/terms/>). After six months it is available under a Creative Commons License (Attribution–Noncommercial–Share Alike 4.0 International license, as described at <https://creativecommons.org/licenses/by-nc-sa/4.0/>).



molecules to facilitate leukocyte passage (Mamdouh et al., 2008).

Isoleucine-glutamine (IQ)-motif containing GTPase activating protein 1 (IQGAP1) was found to be enriched in LBRC-containing membrane fractions as part of a proteomics screen (Sullivan et al., 2014). IQGAP1 is a large, multi-domain scaffolding protein involved in a number of diverse cellular processes including migration and tumorigenesis (Hedman et al., 2015). Structurally, it is composed of six distinct domains. The role for IQGAP1 in TEM has only recently been described (Sullivan et al., 2019). Specifically, both the N-terminal calponin homology domain (CHD) and the IQ domain are required for IQGAP1 function during TEM. The CHD is required to localize IQGAP1 to the junction where it surrounds the transmigrating leukocyte; however, what the IQ domain interacts with and how this facilitates TEM is unknown. Previous studies have shown that the IQ domain can interact with calmodulin (CaM), a ubiquitous calcium-modulating protein, but this interaction in endothelial cells has not been explored (Jang et al., 2011; Li and Sacks, 2003). Ca^{2+} /CaM-dependent protein kinase II (CaMKII) is a common, multifunctional serine/threonine kinase that is regulated by Ca^{2+} /CaM. In endothelial cells, CaMKII δ has been identified as the predominant isoform, but its role during leukocyte TEM has not been investigated (Wang et al., 2010b). The findings presented here demonstrate evidence of highly spatiotemporally localized calcium signaling during TEM in vivo. Furthermore, we establish that the mechanism responsible for transducing this signal to promote TEM during an acute inflammatory response involves IQGAP1, CaM, and CaMKII δ .

Results

Endothelial calcium flux increases locally around transmigrating leukocytes in vivo

Several studies have attempted to characterize in vitro endothelial cell calcium influx during TEM, but none have investigated this process in vivo (Huang et al., 1993; Kielbassa-Schnepp et al., 2001). We sought to examine the spatiotemporal kinetics of calcium in real time during TEM. To visualize dynamic calcium signaling in vivo, we employed intravital microscopy in mice that selectively express the genetically encoded, fluorescent calcium reporter GCaMP3 in endothelial cells using a VE-Cadherin Cre (Tian et al., 2009). In the absence of calcium, GCaMP3 exists in a minimally fluorescent state. However, when calcium binds, it induces a structural change that results in substantially increased fluorescence. This allows GCaMP3 to serve as a calcium indicator and allows for tracking of intracellular calcium dynamics without affecting intracellular calcium concentrations or calcium signaling pathways (Akerboom et al., 2009; Cui et al., 2016; Frommer et al., 2009; Tian et al., 2009).

GCaMP3 VE-Cadherin Cre mice were then used as recipients in an adoptive bone marrow transfer procedure with *CatchUp^{IVM}* (C57BL/6-Ly6G[Cre-tdTomato]) mice as donors (Hasenberg et al., 2015). *CatchUp^{IVM}* mice have red fluorescent protein (tdTomato) under control of the Ly6G locus, which is specifically expressed in neutrophils. Thus, in the chimeric mice, we could

visualize endothelial calcium signal as fluorescence in the green channel and track transmigrating neutrophils using fluorescence in the red channel (Fig. 1 A and Video 1). Mice were injected intrascrotally with an inflammatory stimulus, murine IL-1 β , and with a far red fluorescently conjugated nonblocking anti-PECAM antibody to label the vasculature. We then exteriorized the cremaster muscle to visualize leukocyte-endothelial cell dynamics in real time using a spinning disk confocal microscope (Sullivan et al., 2019, 2016; Watson et al., 2015). Careful replay and rotation of the 4D video images using Volocity software verified that the neutrophils observed had indeed completed TEM. Additionally, to confirm that the adoptive bone marrow transfer did not affect neutrophil function, we performed short-term labeling of neutrophils in naive GCaMP3 VE-Cadherin-Cre mice using an anti-CD18 antibody (Fig. 1 B and Video 2).

Many TEM events were observed from start to finish, and in all of them a rise in endothelial cell calcium concentration was associated with the neutrophil TEM event (Fig. 1, A and B; Video 1; and Video 2). In total, 12 mice with 30 separate fields of view were studied. 66 TEM events were observed. Of these, 55 TEM events (83%) were associated with spatiotemporally correlated calcium signals. TEM events were defined as PECAM pore opening and passage of neutrophils through endothelial cells as visualized by morphology. TEM events were considered to have associated calcium signal if there was at least 15% increase in fluorescence compared with neighboring off-pore background-corrected baseline fluorescence.

While TEM events and their associated calcium signals can frequently be observed, not all events can be quantitated as normalized fluorescence over time, as shown in Fig. 1 C. In particular, when TEM events occur at the side of the post-capillary venule, the associated calcium signal is visualized as a semicircle rather than a complete ring; therefore, these events cannot be properly quantitated and compared with those TEM events that occur en face. Moreover, it can be difficult to capture the entirety of a TEM event from beginning to end. There is often also some heterogeneity in GCaMP expression across endothelial cells of a vessel, and this additionally makes it difficult to capture ideal TEM events.

As neutrophil TEM occurs across endothelial cell junctions, formation of an adjacent PECAM-bordered transmigratory pore can be seen. Concurrently, there is a substantial increase in intracellular endothelial calcium signal ($\uparrow[\text{Ca}^{2+}]_i$) surrounding the neutrophil (Fig. 1, A and B). This indicates that the endothelial calcium signal for TEM is local rather than global. Furthermore, the $\uparrow[\text{Ca}^{2+}]_i$ is specific for the TEM step and is not associated with preceding events such as rolling, adhesion, or locomotion. This increase in fluorescence can be quantified as a distinct peak that occurs over several minutes, with each colored line representing a separate transmigration event (Fig. 1 C). The individual peaks have been adjusted to start at the same point, but the duration of TEM can be slightly variable, so not all peaks end simultaneously. Note that $\uparrow[\text{Ca}^{2+}]_i$ peaked about midway through TEM and fell to at or near baseline before TEM was complete. An axial profile of the calcium signal is shown in Fig. 1 D. This demonstrates that the pore size is several microns in diameter, and this was consistent between several TEM

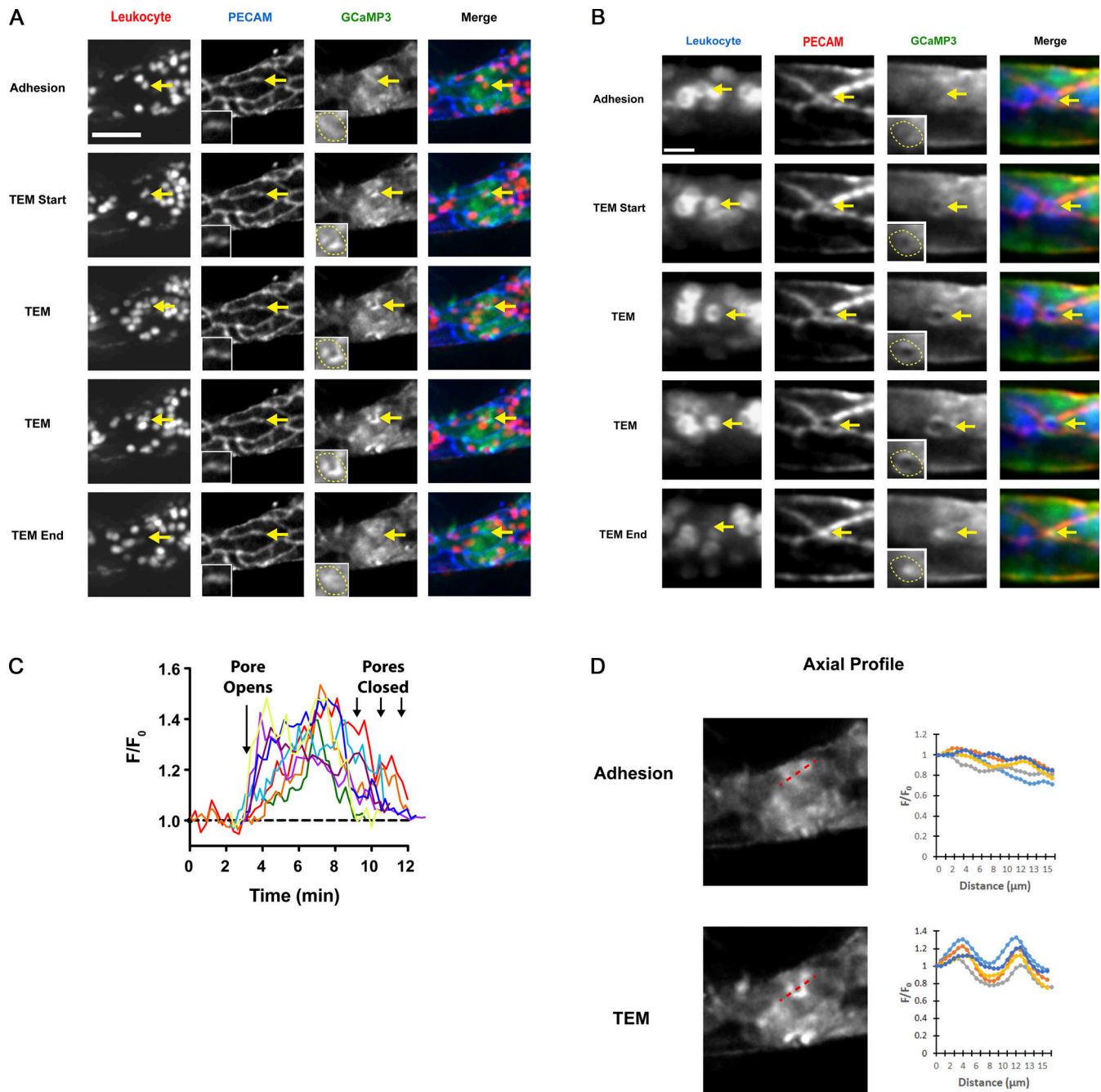


Figure 1. Local endothelial cell calcium influx is associated with in vivo neutrophil TEM. (A) Mice expressing the calcium sensor GCaMP3 specifically in endothelial cells (VE-Cadherin Cre GCaMP3^{fl/fl}) were lethally irradiated and their bone marrow reconstituted from *CatchUp*^{VM} with red fluorescent neutrophils. After allowing reconstitution, inflammation was induced by intrascrotal injection of IL-1 β . Nonblocking fluorophore-conjugated anti-PECAM (blue) was also coinjected to visualize the vasculature. 4 h after the injection, the cremaster muscle was exteriorized and prepared for confocal intravital microscopy as detailed in the Materials and methods. The images shown are Z-projections of the 3D stacks. A full-length video is included in the supplemental material (Video 1). Arrows denote neutrophils in the process of TEM. Endothelial cell calcium influx is associated with neutrophil TEM and is localized around the trans migratory pore. Insets display a magnified view of the local PECAM pore and calcium influx. 12 mice were studied. Scale bar is 50 μm . (B) Inflammation was induced in VE-Cadherin Cre GCaMP3^{fl/fl} mice by intrascrotal injection of IL-1 β . Nonblocking fluorophore-conjugated anti-PECAM (red) and fluorescently conjugated anti-CD18 (blue) were coinjected to visualize the vasculature and circulating neutrophils, respectively. This additional approach provided validation of our adoptive bone marrow transfer model. 4 h after the injection, the cremaster muscle was exteriorized and prepared for confocal intravital microscopy as detailed in the Materials and methods. The images shown are Z-projections of the 3D stacks. A full-length video is included in the supplemental material (Video 2). Arrows denote neutrophils in the process of TEM. Endothelial cell calcium influx is associated with neutrophil TEM and is localized around the trans migratory pore. Insets display a magnified view of the local calcium influx. Scale bar is 10 μm . (C) Each colored line represents a separate transmigration event where the calcium signal was quantitated. Mean fluorescence intensity of the region of interest (dotted lines in A and B) was calculated, background corrected, and normalized to baseline as described in the Materials and methods. The beginning and completion of TEM were defined by the PECAM gap. Eight independent TEM events are shown here. (D) Intravital microscopy videos of inflammation in mice expressing the calcium sensor GCaMP3 restricted to

endothelial cells were analyzed. For axial profile analysis, a 15- μ m line (shown as the dotted red line) was drawn centered on the pore of a TEM event, and the pixel intensity along that line was recorded for the green channel (GCaMP3 signal). The same line was used to analyze pixel intensity for the GCaMP3 signal when the leukocyte was adherent to the endothelium before the TEM event. The individual lines were adjusted slightly to account for variations in the center of the pore. The plots were normalized to the minimum intensity value proximal to the pore. Note that this makes the relative intensities for the plots similar at the proximal 0- μ m end of the plot, but retains meaningful information regarding the axial profile of the GCaMP3 signal. Five separate TEM events are shown here.

events and with previous reports (Heemskerk et al., 2016; Mamdouh et al., 2009; Nourshargh and Alon, 2014). This is the first live, in vivo characterization of endothelial cell calcium dynamics during TEM and demonstrates that the increase in endothelial cytosolic free calcium is highly localized near the transmigratory pore.

CaM interacts with the IQ domain of IQGAP1 in endothelial cells

To understand the molecular signaling events that occur during TEM after the local calcium influx, we made use of rigorously controllable in vitro models. IQGAP1 was identified as a potential actor in the TEM pathway through a screen for LBRC-associated proteins (Sullivan et al., 2014). We recently confirmed that it is required for TEM and identified the CHD and IQ domain as being crucial for this function (Sullivan et al., 2019). The CHD is required to bring IQGAP1 to the endothelial cell border; the function of the IQ domain is not known. The IQ domain has been shown to interact with CaM, but this interaction has not been demonstrated in human endothelial cells (Li and Sacks, 2003). To investigate the mechanism by which the IQ domain facilitates TEM, we examined its ability to interact with CaM using two previously characterized IQGAP1 domain truncation mutants. These mutants contained a C-terminal GFP tag and were designed to differ only by the presence of the IQ domain (Fig. 2 A). Construct Δ 5,6 is the minimal motif of IQGAP1 required for TEM. It rescues the TEM defect caused by endogenous IQGAP1 knockdown; it contains both the CHD and IQ domains. Construct Δ 4-6 lacks the IQ domain (domain 4) and therefore does not support TEM, even though it localizes to the cell border (Sullivan et al., 2019).

The ability of constructs Δ 5,6 and Δ 4-6 to bind CaM in endothelial cells was studied with a CaM Sepharose pull-down assay. Endogenous full-length IQGAP1 and construct Δ 5,6 bound to CaM both in the presence and absence of calcium. In contrast, construct Δ 4-6 did not bind CaM in either the presence or the absence of calcium (Fig. 2 B). This indicates that the IQ domain of IQGAP1 is indeed necessary for facilitating an interaction with CaM in human endothelial cells.

CaM function in endothelial cells is required for TEM

To investigate the role of CaM and its downstream binding partner, CaMKII, in TEM, we used trifluoperazine (TFP) and KN-93 to pharmacologically inhibit CaM and CaMKII function, respectively. TFP is a CaM antagonist that inactivates Ca²⁺/CaM (Vandonselaar et al., 1994). KN-93 is a widely used CaMKII antagonist that prevents CaMKII activation by competing for binding with Ca²⁺/CaM (Brooks and Tavalin, 2011; Wong et al., 2019). Cytokine-activated endothelial cell (immortalized human umbilical vein endothelial cell [iHUVEC]) monolayers were

pretreated with either 100 μ M TFP or 10 μ M KN-93 for 30 min. Monocyte TEM was subsequently assessed using a standard TEM assay. Under control untreated conditions, 83% of monocytes were able to transmigrate. However, when endothelial cells were pretreated with TFP or KN-93, TEM was reduced significantly to 15% and 23%, respectively (Fig. 3 A).

Using the CaM Sepharose pull-down assay, we also established the interaction between CaM and CaMKII δ specifically in endothelial cells. As reported by others, we were able to confirm that the δ isoform of CaMKII is abundant and readily detectable in endothelial cells (Wang et al., 2010b). Furthermore, the interaction between CaM and CaMKII δ is calcium dependent. In the absence of calcium, there is no interaction; however, in the presence of calcium, there is a significant interaction (Fig. 3 B). This interaction can be attenuated if the endothelial cells are pretreated with KN-93, suggesting that this is the mechanism by which KN-93 inhibits TEM. These results are further consistent

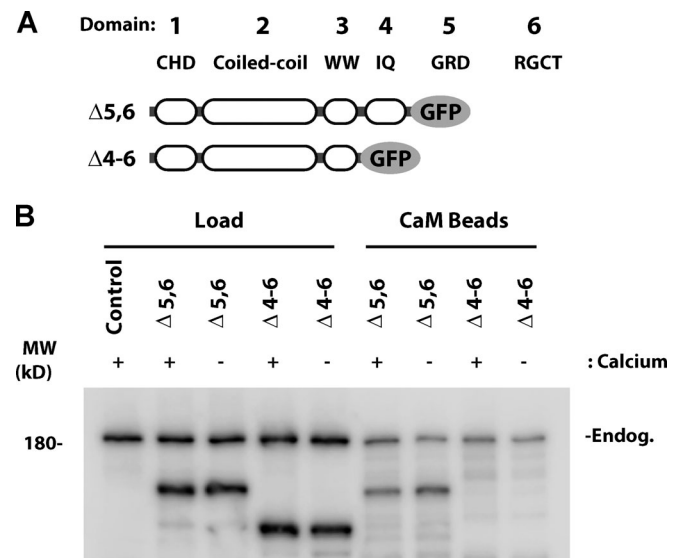


Figure 2. The IQ domain of IQGAP1 interacts with CaM in endothelial cells. (A) Schematic showing the two IQGAP1 domain truncation constructs fused to GFP. GRD, RasGAP-related domain; IQ, IQ motifs domain; RGCT, RasGAP C-terminus; WW, tandem tryptophan-containing domain. **(B)** The GFP-tagged IQGAP1 domain truncation constructs shown in A were transduced into iHUVECs grown on 60-mm tissue culture plates. After 2 d of expression, the cells were lysed in either the presence of CaCl₂ or EGTA. The protein lysates were then incubated with CaM Sepharose beads, and the beads were then eluted in 6 \times Laemmli buffer to be probed using Western blotting as described in the Materials and methods. The blot shown here was probed for IQGAP1. Both endogenous (Endog.) full-length IQGAP1 and construct Δ 5,6 interact with CaM. However, construct Δ 4-6, which lacks the IQ domain, cannot bind CaM in either the presence or the absence of calcium. Three separate experiments were performed. MW, molecular weight.

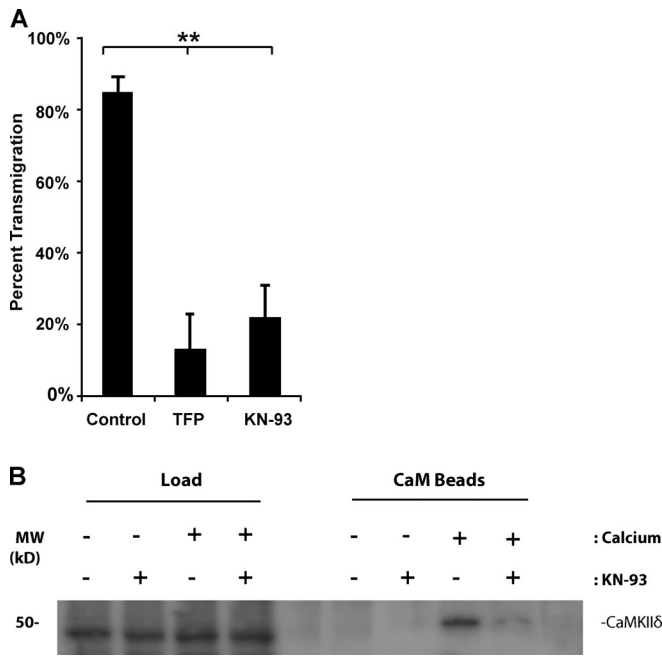


Figure 3. CaM interacts with CaMKIIδ in the presence of calcium and inhibiting CaM, or CaMKII activity significantly reduces monocyte TEM. (A) Monocyte transmigration across iHUVCEs pretreated with either 100 μM TFP or 10 μM KN-93 is substantially reduced when compared with monocyte transmigration across untreated iHUVCE monolayers. Data represent the average and standard deviation of three independent experiments. Each experiment comprises at least two samples with >50 leukocytes scored per sample for each condition. ** denotes P value < 0.01 with Student's *t* test. (B) iHUVCEs grown on 60-mm tissue culture plates were left untreated or were treated with 10 μM KN-93 for 30 min as described in the Materials and methods. After extensive washing, the endothelial cells were lysed in the presence of either CaCl₂ or EGTA. The protein lysates were then incubated with CaM Sepharose beads, and the beads were eluted in 6× Laemmli buffer to be probed using Western blotting as described in the Materials and methods. The blot shown here was probed for CaMKIIδ. CaMKIIδ interacts with CaM in the presence of calcium but not in the absence of calcium. Furthermore, the interaction between CaM and CaMKIIδ even in the presence of calcium can be attenuated by pretreating with KN-93, and this also prevents monocyte transmigration as shown in A. Three separate experiments were performed. MW, molecular weight.

with a model wherein CaM binding to CaMKIIδ is a key signaling event downstream of the calcium influx needed to support TEM.

Inhibiting endothelial CaMKII function blocks TEM

To overcome limitations in specificity associated with pharmacologic inhibition and to more directly assess the role of CaMKII during TEM, we expressed a hemagglutinin (HA)-tagged CaMKII inhibitor peptide (CaMKIIN; Chang et al., 2001; Murthy et al., 2017) in endothelial cells. CaMKIIN was detected at its predicted apparent molecular weight (Fig. 4 A), and its expression was also validated using fluorescence microscopy (Fig. 4 B). The construct is primarily localized to the cytoplasm. Note that endothelial cell morphology in general and VE-cadherin expression and distribution in particular are not affected. Under control conditions with empty virus, 58% of monocytes underwent transmigration. However, monocyte TEM across endothelial cells expressing CaMKIIN was reduced significantly, and

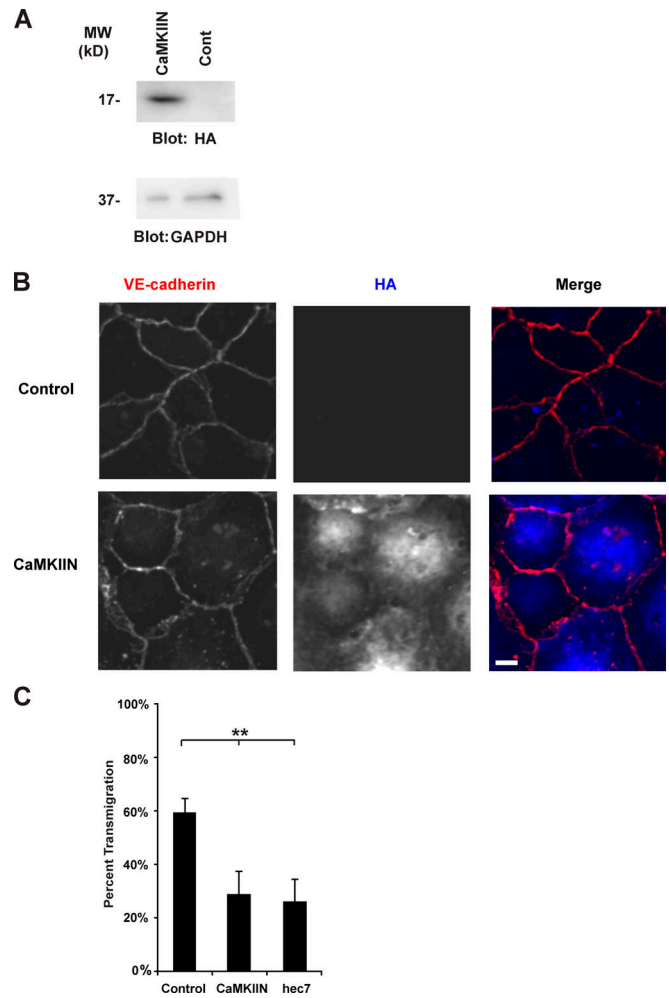


Figure 4. A small peptide inhibitor of CaMKII substantially reduces monocyte TEM. (A) iHUVCEs were transduced with CaMKIIN. 2 d after transduction, cells were lysed and their protein content resolved using SDS-PAGE and probed with Western blotting. Control (Cont) is shown for reference. GAPDH is shown as the loading control. (B) iHUVCEs were fixed, permeabilized, stained for HA and VE-cadherin, and visualized using confocal immunofluorescence microscopy. Scale bar is 10 μm. (C) Monocyte transmigration across iHUVCEs grown on collagen gels transduced with CaMKIIN is shown. The mouse anti-human PECAM antibody hec7 was included as a control. Data represent the average and standard deviation of three independent experiments. Each experiment comprises at least three samples with >50 leukocytes scored per sample for each condition. ** denotes P value < 0.01 with Student's *t* test. MW, molecular weight.

only 29% of monocytes were able to transmigrate. This is comparable to the level of blockade observed when PECAM interactions were disrupted with the mouse anti-human PECAM antibody hec7, where 26% of monocytes transmigrated (Fig. 4 C).

Dominant negative CaMKIIδ blocks TEM

Next, we specifically disrupted endothelial cell CaMKIIδ (the predominant isoform in endothelial cells) function to determine whether this isoform is crucial for TEM. For this we used an HA-tagged dominant negative CaMKIIδ construct that contains an amino acid substitution (K43A) to prevent ATP binding, rendering it kinase dead (Pfleiderer et al., 2004; Rich and Schulman,

1998). We detected expression of dominant negative CaMKII δ at its predicted molecular weight (Fig. 5 A), and its expression was also validated using fluorescence microscopy (Fig. 5 B). Similar to the localization pattern of CaMKIIN, dominant negative CaMKII δ also predominantly localized to the cytoplasm, and similarly, there was no effect on endothelial cell morphology or VE-cadherin expression. In the TEM assay, dominant negative CaMKII δ significantly inhibited transmigration. 72% of monocytes underwent transmigration under control conditions with empty virus; however, only 29% of monocytes underwent TEM when dominant negative CaMKII δ was expressed in endothelial cells (Fig. 5 C). Again, this degree of blockade was comparable to what was observed with an anti-PECAM, or *hec7*, block where 24% of monocytes transmigrated. These data identify CaMKII δ as a major endothelial signaling molecule involved in TEM.

CaMKII δ targets the LBRC to the transmigrating leukocyte

It was previously shown that during TEM, delivery of the LBRC membrane to the migrating leukocyte occurs. This process, called targeted recycling, is essential for facilitating leukocyte passage. To understand the mechanism of how dominant negative CaMKII δ blocks leukocyte TEM, we wanted to investigate its effect on targeted recycling of LBRC in endothelial cells. For this, a validated targeted recycling assay that detects recycling LBRC membrane as fluorescence enrichment surrounding transmigrating leukocytes was performed (Mamdouh et al., 2003, 2008, 2009). Expression of dominant negative CaMKII δ did not affect the ability of monocytes to localize to the junctions (Fig. 6 B). However, consistent with its ability to inhibit TEM, there was a significant reduction in targeted recycling of LBRC in the endothelial cells expressing dominant negative CaMKII δ that was proportional to the reduction in TEM (compare Fig. 5 B and Fig. 6 B). Under control conditions, 54% of monocytes had enriched fluorescence signal indicative of targeted recycling of the LBRC (Fig. 6 A). On the other hand, only 23% of monocytes on CaMKII δ dominant negative monolayers had enriched fluorescence adjacent to the infiltrating monocytes (Fig. 6 B). These findings suggest that CaMKII δ is critical for mediating targeted recycling of the LBRC to surround leukocytes during TEM.

Inhibiting endothelial CaMKII in vivo blocks TEM

To corroborate our in vitro findings regarding the role of CaMKII in TEM and further explore the pathophysiologic relevance of this calcium signaling pathway in vivo, we generated a line of tamoxifen inducible VE-Cadherin Cre CaMKIIN mice. These mice express CaMKIIN, the peptide inhibitor that blocked TEM when tested in vitro (Fig. 3), selectively in endothelial cells in the presence of tamoxifen. This allowed us to study the effect of inhibiting CaMKII in endothelial cells without affecting CaMKII function during development or in other cell types such as leukocytes.

After inducing CaMKIIN expression with tamoxifen, we examined TEM using the croton oil dermatitis model of acute inflammation (Sullivan et al., 2016; Watson et al., 2015; Weber et al., 2015). In this assay, croton oil, a strong irritant and inflammatory stimulus, is applied topically to both leaflets of one mouse ear for 5 h, after which the animals are sacrificed and

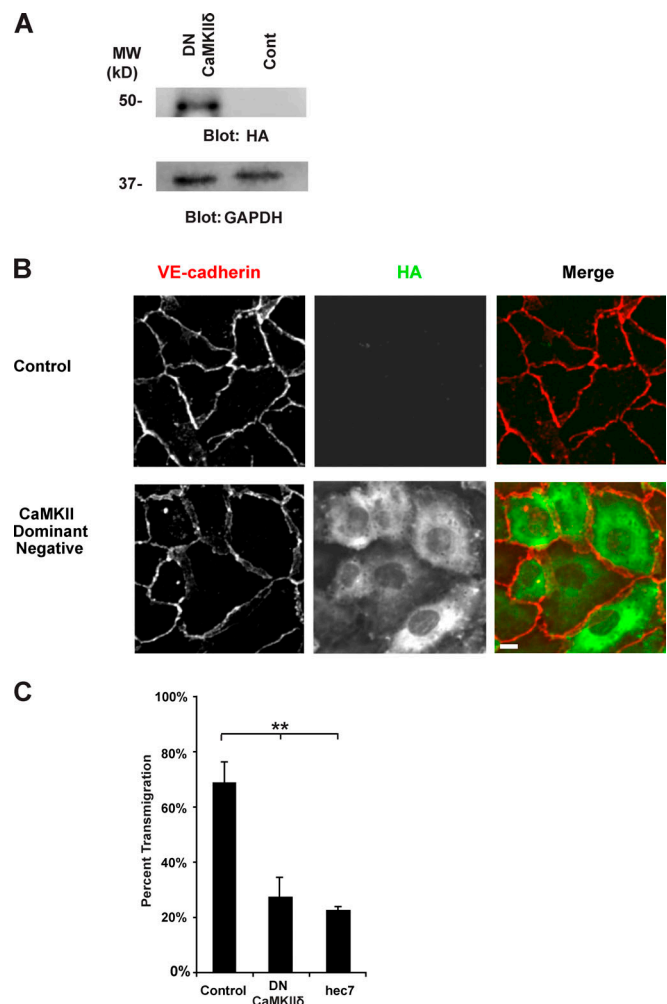


Figure 5. Dominant negative CaMKII δ markedly reduces monocyte TEM. (A) iHUEVCs were transduced with dominant negative CaMKII δ . 2 d after transduction, cells were lysed and their protein content resolved using SDS-PAGE and probed with Western blotting. Control (Cont) is shown for reference. GAPDH is shown as the loading control. (B) iHUEVCs were fixed, permeabilized, stained for HA and VE-cadherin, and visualized using confocal immunofluorescence microscopy. Scale bar is 10 μ m. (C) Monocyte transmigration across iHUEVCs grown on collagen gels and transduced with dominant negative (DN) CaMKII δ is shown. The mouse anti-human PECAM antibody *hec7* was included as a control. Data represent the average and standard deviation of three independent experiments. Each experiment comprises at least three samples with >50 leukocytes scored per sample for each condition. ** denotes P value < 0.01 with Student's *t* test. MW, molecular weight.

their ears are harvested for staining and immunofluorescence microscopy (Fig. 7 A). Immunofluorescence confirmed the presence of HA-tagged CaMKIIN in endothelial cells (Fig. S1). However, since enhanced GFP (eGFP) is expressed in all cells that have not undergone Cre recombination, the green channel could not be used for experimentation. Therefore, the ears were stained for endothelial cells using anti-PECAM (clone 2H8) conjugated to DyLight 550, and neutrophils were stained using rat anti-mouse MRP14 directly conjugated with DyLight 649.

Neutrophil position with respect to the endothelial cells was precisely scored according to a standard system (Fig. 7 B; Sullivan

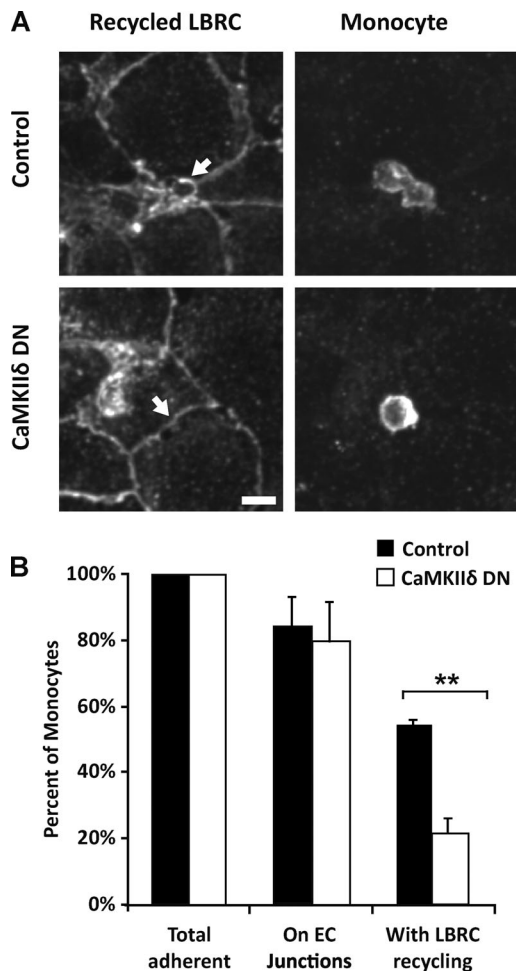


Figure 6. CaMKII δ is required for targeted recycling of the LBRC. (A) iHUVCEs grown on collagen gels and transduced with dominant negative (DN) CaMKII δ as in Fig. 4 were subjected to the targeted recycling assay (described in the Materials and methods). This assay follows the recruitment of the LBRC to the site of transmigration. Using immunofluorescence microscopy, recycled LBRC is visualized as increased fluorescence adjacent to transmigrating monocytes. The arrow in the control panel highlights LBRC recruitment adjacent to the transmigrating monocyte while the arrow in the dominant negative panel highlights the notable absence of LBRC recruitment. Images shown here are representative of three independent experiments. Scale bar is 10 μ m. **(B)** Quantification of the monocyte position and LBRC recruitment shown in A. Monocytes were considered at the junction if they overlapped at all with the endothelial cell (EC) junctions in the x-y plane. Data shown here are the average and standard deviation of three independent experiments. Each experiment had at least 50 monocytes scored. Data from each experiment were normalized to the total adherent cells to account for subtle differences in adhesion on each monolayer. ** denotes P value < 0.01 with Student's *t* test.

et al., 2019; Watson et al., 2015; Weber et al., 2015). Both control and CaMKIIN-expressing mice recruited similar numbers of neutrophils to the ear (Fig. 7 C). The majority of neutrophils in control mice were observed outside the blood vessels in the inflamed tissue. However, mice expressing CaMKIIN in their endothelial cells showed a significant reduction in the number of neutrophils observed outside the vessel, with a corresponding increase in the number of neutrophils observed arrested inside the vessel on the apical surface (Fig. 7 D).

Deleting endothelial CaMKII δ in vivo prevents TEM

Although these findings support a role for calcium signaling, specifically through CaMKII in vivo, we wanted confirmation using a second model that also allowed us to examine the role of endothelial CaMKII δ . To do this, we derived a novel, endothelial cell-specific CaMKII δ deletion mouse model. In this model, CaMKII δ was deleted from endothelial cells when VE-cadherin Cre expression was induced with tamoxifen (Fig. S2). We then studied the ability of these mice to respond to an acute inflammatory stimulus in the croton oil dermatitis model as described above. Ears were then harvested, and the leaflets were stained for endothelial cells, neutrophils, and basement membranes. Again, the position of neutrophils was quantified using a standardized scoring system, but here the addition of the basement membrane stain helped more clearly delineate whether leukocytes were arrested in the perivascular space or whether they were outside the basement membrane (Fig. 8, A and B). Again, similar numbers of neutrophils were able to adhere (Fig. 8 C). Under control conditions, in which endothelial cells expressed CaMKII δ , the majority of neutrophils were found outside the blood vessels (Fig. 8, A and D). However, in mice lacking endothelial expression of CaMKII δ , the majority of neutrophils remained arrested apically within postcapillary venules, with a significant reduction in the number of cells able to exit the blood vessels (Fig. 8 D).

Discussion

The data presented here show for the first time that endothelial cell calcium signaling is spatiotemporally restricted during TEM. Using a novel intravital imaging platform with endothelial-specific GCaMP3 mice enables real-time quantification of endothelial cell calcium influx during TEM in high spatiotemporal resolution. As a transmigration pore is formed and transmigration begins, there is a substantial increase in cytosolic endothelial calcium signal surrounding the migrating leukocyte. The calcium signal peaks approximately midway through the transmigration process and returns to at or near baseline when the leukocyte has completed transmigration and the PECAM pore closes. Importantly, this calcium influx is distinct from the calcium requirements at other steps in the inflammatory cascade, such as rolling and adhesion. There is no enrichment of calcium signal at endothelial cell junctions until immediately before the initiation of transmigration.

There are, however, other calcium transients that we observed that are morphologically distinct from TEM and do not occur temporally or spatially with TEM. In particular, we frequently observed that footprint-like calcium signals correlated with neutrophils that have transmigrated and are positioned below the endothelium. Neutrophils crawl along the basolateral side of the endothelium for several minutes before ultimately migrating across the basement membrane (Proebstl et al., 2012; Song et al., 2017). This generates a distinct, mobile pattern that is easily differentiated from a true TEM event. We believe that this distinct calcium signal arises from assembly and disassembly of focal adhesions between endothelial cells and the basement membrane, as this process was previously shown to cause discrete increases in endothelial calcium (Giannone et al., 2004).

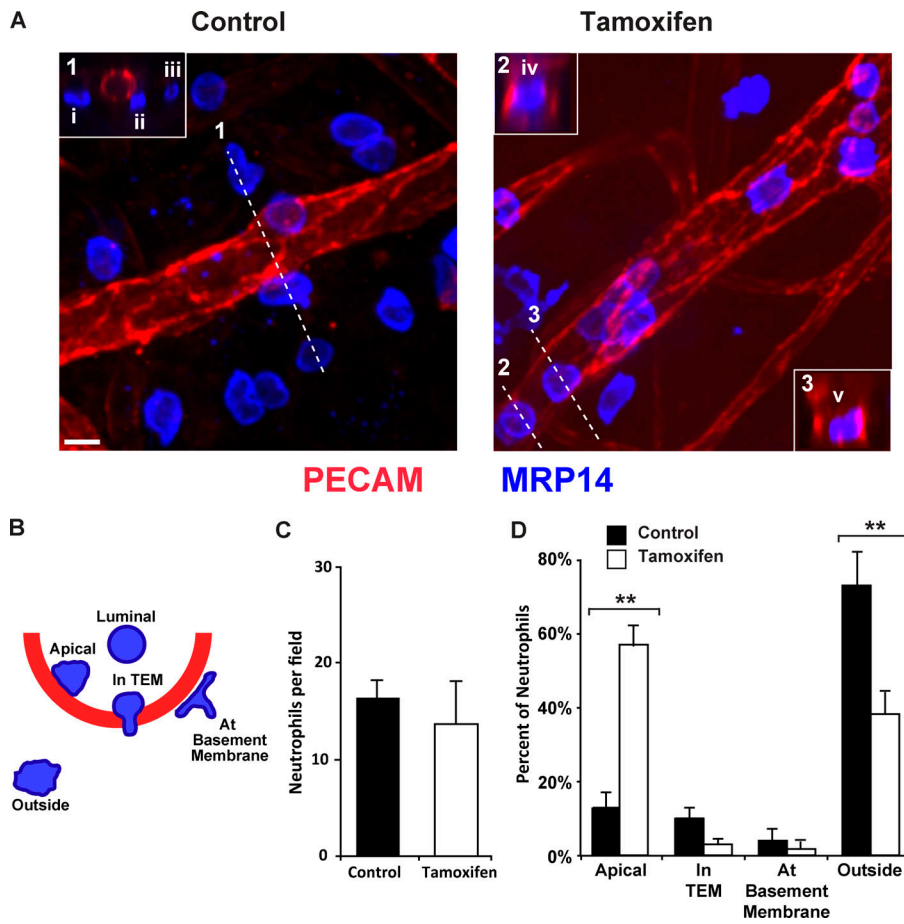


Figure 7. Inhibiting CaMKII in vivo significantly reduces neutrophil TEM. (A) iVE-Cre CaMKIIN^{f/f} mice were injected for 5 d consecutively with either tamoxifen or corn oil (control) as described in the Materials and methods. After allowing for a 1-wk recovery period, one ear of each mouse was treated topically with croton oil in an acetone:olive oil carrier while the other ear was treated topically with carrier alone. After 5 h, the mice were sacrificed and their ears were processed for immunofluorescence imaging using confocal microscopy on whole-mount specimens. Representative images from control and CaMKIIN-expressing (tamoxifen-injected) mice are shown. Neutrophils and endothelial cell junctions were visualized with antibodies against MRP14 (blue) and PECAM (red), respectively. Insets show the orthogonal view at the position denoted by the dashed line. Orthogonal inset 1 shows three leukocytes (i–iii) outside the blood vessel. Orthogonal insets 2 and 3 show two leukocytes arrested on the apical surface (iv and v). Scale bar is 10 μ m. (B) Schematic of the neutrophil positional scoring system used to quantify the locations of neutrophils observed in A. (C) Quantification of the total number of neutrophils per field. Data shown are the average and standard deviations of the three independent experiments. Only neutrophils within 50 μ m of the vessel were scored. (D) Quantification of the leukocyte positions from the images collected in A. Data shown are the average and standard deviations from three separate experiments. At least five fields with at least 100 neutrophils for each mouse were analyzed. Data shown do not include data for the neutrophils found in the luminal position. ** denotes P value < 0.01 with Student's *t* test. Carrier-only ears showed no signs of inflammation, and neutrophils were rarely found in the tissue or associated with the vessels (data not shown).

We considered the possibility that the increase in fluorescence intensity during TEM is due to changes in cellular morphology surrounding the transmigratory pore; however, we believe this is unlikely. When quantifying fluorescence surrounding transmigrating neutrophils, we selected a region larger than and inclusive of the pore rather than simply quantifying the fluorescence of the ring itself. If there were only local redistribution of cytoplasm, the total amount of fluorescence signal over this larger area would remain unchanged over time. This is not what we observed. In addition, we observed no decrease in GFP intensity adjacent to the transmigratory pore. Since endothelial cells are extremely thin (<1 μ m at the junctions), if there were a substantial shift in local cytoplasmic volume, it would likely come from nearby cytoplasm. This would be reflected by a respective decrease in adjacent GFP intensity that corresponded to the respective increase in GFP intensity at the TEM pore. This was not the case. For these reasons, we believe it is unlikely that local changes in cellular morphology account for the increase in fluorescence intensity.

Ideally, we would perform an experiment to visualize the TEM of fluorescent neutrophils across endothelial cells expressing

calcium-insensitive eGFP uniformly throughout the cytoplasm. In such experiments, cytoplasmic rearrangement or changes in local endothelial cell thickness during TEM would be visualized as increases in eGFP fluorescence intensity. However, if our hypothesis is correct and the increased fluorescence intensity we see in the GCaMP3 mice is due to $\uparrow[Ca^{2+}]_i$ rather than change in cellular morphology, we would not see a significant increase in eGFP fluorescence intensity associated with TEM in mice expressing calcium-insensitive eGFP. Unfortunately, due to restrictions on research laboratory operations at the time of this writing caused by the global COVID-19 pandemic, we have been unable to perform such experiments, and it remains uncertain when restrictions will be lifted. Nonetheless, for the reasons outlined in the previous paragraph, we believe that our interpretation of the data is correct.

Previous work has shown that the absence of TRPC6 from murine endothelial cells results in a luminal arrest of neutrophils in a croton oil dermatitis model of inflammation (Dalal et al., 2020; Weber et al., 2015). However, this was a static assay with fixed tissues and did not address the endothelial calcium dynamics that occur during TEM. Furthermore, published data

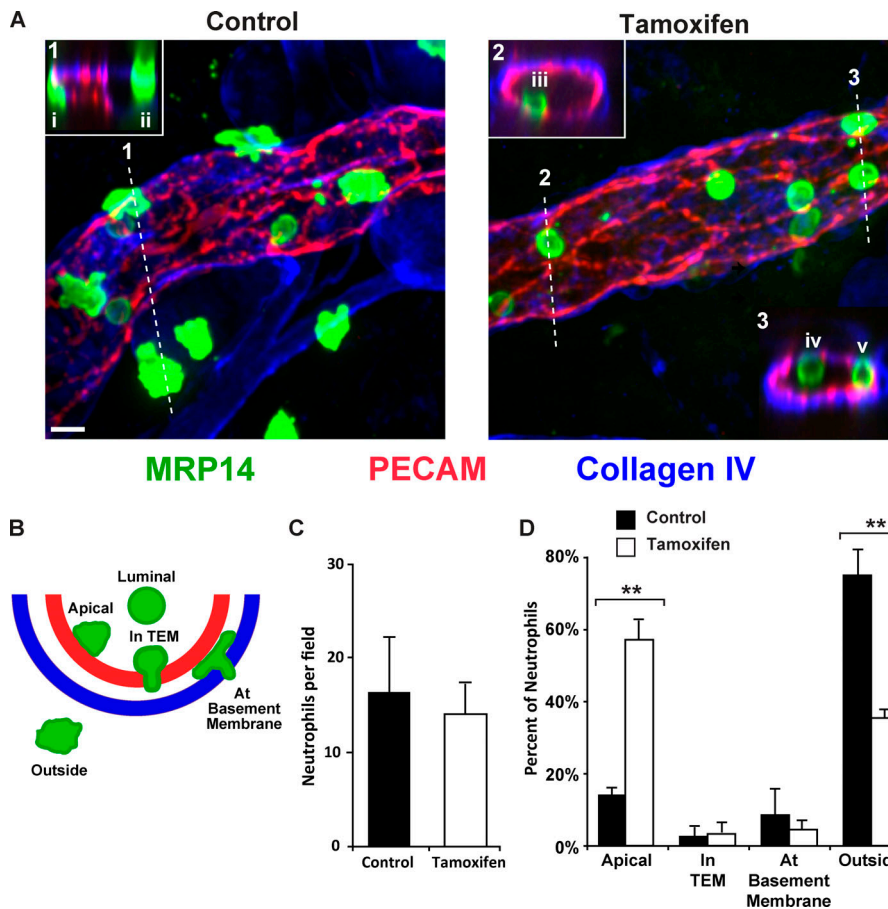


Figure 8. CaMKII δ is required for neutrophil TEM in vivo. (A) iVE-Cre CaMKII $\delta^{fl/fl}$ mice were injected for 5 d consecutively with either tamoxifen or corn oil as described in the Materials and methods. After allowing for a 1-wk recovery period, one ear of each mouse was treated topically with croton oil in an acetone:olive oil carrier while the other ear was treated topically with carrier alone. After 5 h, the mice were sacrificed and their ears processed for immunofluorescence imaging using confocal microscopy. Representative images from control and endothelial cell CaMKII δ knockout mice are shown. Here, neutrophils, endothelial cell junctions, and basement membranes were visualized with antibodies against MRP14 (green), PECAM (red), and collagen IV (blue), respectively. Insets show the orthogonal view at the position denoted by the dashed line. Orthogonal inset 1 shows two leukocytes (i and ii) outside the blood vessel and basement membrane. Orthogonal insets 2 and 3 show three leukocytes arrested on the apical surface (iii–v). Scale bar is 10 μ m. (B) Schematic of the neutrophil positional scoring system used to quantify the locations of neutrophils observed in A. (C) Quantitation of the total number of neutrophils per field. Only neutrophils within 50 μ m of the vessel were scored. Data shown are the average and standard deviations of the three independent experiments. (D) Quantitation of the leukocyte positions from the images collected in A. Data shown are the average and standard deviations collected from three separate experiments. At least five fields with at least 100 neutrophils for each mouse were analyzed. Data shown do not include data for the neutrophils found in the luminal position. ** denotes P value <0.01 with Student's *t* test. Carrier-only ears showed no signs of inflammation, and neutrophils were rarely found in the tissue or associated with the vessels (data not shown).

performed in vitro by loading endothelial cells with a calcium imaging dye seemed to show that endothelial cells undergo global calcium influx during TEM (Su et al., 2000). This model does not fully recapitulate the complexities of leukocyte transmigration, and there have been no studies reproducing this observation in vivo. Duza and Sarelius (2004) studied endothelial cell calcium transients in arterioles in vivo by perfusing mice with a calcium indicator. However, there was no attempt to study TEM with this system. Our unique findings demonstrate that dissecting the spatiotemporal characteristics of calcium changes in real time can help develop better models of endothelial cell function and advance our understanding of calcium signaling patterns in both healthy and dysfunctional endothelium.

We previously showed that three major molecules regulating this process, namely PECAM (Mamdouh et al., 2003; Muller et al., 1993), TRPC6 (Weber et al., 2015), and IQGAP1 (Sullivan et al., 2019, 2014), are enriched at the site of the migrating leukocyte. Our previous data suggested that the CHD helps enrich IQGAP1 at the junction. In combination with the data

presented here, we show that CaM, which is constitutively bound to IQGAP1 through the IQ domain (Ho et al., 1999), is important in TEM. Once leukocyte PECAM engages endothelial cell PECAM, local TRPC6 activation leads to a calcium influx surrounding the transmigrating leukocyte (Weber et al., 2015). This local influx allows CaM to bind calcium and then activate CaMKII δ , the predominant isoform of CaMKII expressed in endothelial cells, to mediate targeted delivery of the LBRC to facilitate TEM (Fig. 9). Without proper delivery of the LBRC, the leukocyte and endothelial cell lack additional membrane, unligated receptors, and the necessary signals required for TEM (Mamdouh et al., 2003; Muller, 2011).

Mechanistically, we report that the IQ domain of IQGAP1, which is required for TEM, interacts with CaM in endothelial cells. While the IQ domain was previously shown to interact with CaM, this interaction was only shown in MCF-7 (Li et al., 1999) and CV-1 in origin and carrying SV40 (COS) cells (Li and Sacks, 2003). Although the interaction between IQGAP1 and CaM can occur in both the presence and the absence of calcium, the interaction between CaM and CaMKII δ only occurs in the

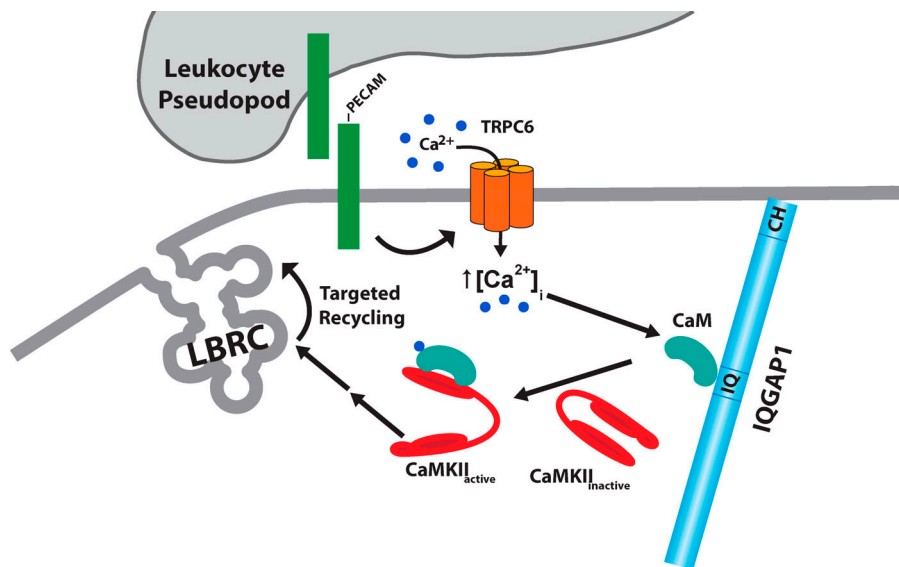


Figure 9. Schematic illustrating mechanism of endothelial cell calcium signaling during TEM. The endothelial cell calcium signaling pathway is activated by homophilic PECAM-PECAM interactions. This leads to activation of TRPC6 and an influx of calcium. The CHD helps enrich IQGAP1 at the junction, allowing CaM bound to the IQ domain to be locally concentrated for the calcium influx. The local influx of calcium allows CaM to then activate CaMKII δ . CaMKII δ subsequently mediates targeted delivery of the LBRC to facilitate TEM. Note that CaMKII is shown as a monomer for clarity.

presence of calcium. This further supports our model where an acute, local calcium influx initiates signal transduction through IQGAP1, CaM, and CaMKII to support TEM.

Inhibiting either CaM or CaMKII δ by a variety of methods both in vitro and in vivo blocks leukocyte TEM, a novel finding that implicates these molecules as critical mediators of the acute inflammatory response. Monocyte TEM in vitro is substantially reduced when endothelial cells are pretreated with TFP or KN-93. Furthermore, KN-93 attenuates the interaction between CaM and CaMKII δ . We additionally confirmed the role of CaMKII by expressing a small peptide inhibitor (CaMKIIN) and dominant negative CaMKII δ in endothelial cells, both of which significantly reduced monocyte transmigration in vitro. Mechanistically, CaMKII δ is required for efficient targeted recycling of the LBRC to migrating leukocytes. This helps us understand calcium signaling as it sequentially relates to other molecules required for TEM, such as CD99. CD99 is not required for the initiation of the targeted recycling of the LBRC but rather is required for subsequent, continuous recruitment of the LBRC (Watson et al., 2015). Since dominant negative CaMKII δ substantially reduced even the initiation of targeted recycling, we conclude that calcium, CaM, and CaMKII δ are required for steps upstream of CD99.

Furthermore, we generated two novel mouse models. This is the first description of an inducible, endothelial-specific CaMKII δ deletion mouse model. Previous studies have used global CaMKII δ knockout mice and cardiomyocyte-specific CaMKII δ knockout mice, but our model uniquely assesses the contribution of endothelial CaMKII δ to disease pathology (Ling et al., 2013, 2009; Suetomi et al., 2018; Willeford et al., 2018). Additionally, in our model CaMKII δ deletion can be induced when the mouse reaches adulthood. This temporally limited approach allows for targeted study of CaMKII δ function without affecting development and limits potential compensation by up-regulation of other CaMKII isoforms.

While determining the relevant substrates of CaMKII δ in regulating TEM is beyond the scope of this study, potential

targets are likely in the vicinity of the LBRC. An elegant study in neurites showed that even though CaMKII and one of its substrates (vimentin) were distributed throughout the neurite cytoplasm, CaMKII-dependent phosphorylation of vimentin occurred only in the region of high calcium (Inagaki et al., 1997). Thus, CaMKII δ activation likely occurs near the transmigration pore when there is a local influx of calcium. CaMKII δ may be involved in affecting cytoskeletal rearrangements through potential interactions with vimentin or kinesin light or heavy chain (Cyrus and Muller, 2016), or it may be involved in affecting calcium influx through a potential interaction with TRPC6, creating a local feedback loop to modulate the calcium signal (Boulay, 2002; Eriksson et al., 2004; Guillaud et al., 2008; Inagaki et al., 1997; Tang et al., 2001; Zhang et al., 2001). Ultimately, further work will be required to determine which of these downstream effectors are involved in facilitating targeted recycling and TEM.

Establishing the importance of CaMKII in leukocyte TEM also uncovers a novel potential target for therapeutic intervention in inflammatory conditions. For example, while bosutinib was originally developed as a Bcr-Abl tyrosine kinase inhibitor for use in chronic myelogenous leukemia, studies have found that it can bind and inhibit CaMKII (Chao et al., 2011). CaMKII is also a target in cardiovascular disease, and several attempts have been made to create selective inhibitors for therapeutic applications (Pellicena and Schulman, 2014). With proper optimization, it may be possible to target CaMKII to reduce aberrant inflammation. Many biological functions rely on local calcium signaling, and this mechanism in endothelial cells specifically allows for the local propagation of calcium signals to facilitate TEM without affecting other cellular functions.

Materials and methods

Antibodies and reagents

Mouse anti-human PECAM IgG_{2a} (clone hec7; Muller et al., 1989), mouse anti-human VE-cadherin IgG_{2a} (clone hec1; Ali

et al., 1997), Armenian hamster anti-mouse PECAM (clone 2H8; Schenkel et al., 2004), and mouse anti-human CD18 (clone IB4; Wright et al., 1983) were produced in the laboratory using standard hybridoma antibody production and purification methods. The nonfunction blocking mouse anti-human PECAM antibody (clone P1.1; Liao et al., 1997) was purified from ascites generously gifted by Peter Newman (Blood Center of Wisconsin, Milwaukee, WI). This was then digested to F(ab) fragments using standard protocols. Mouse anti-human β -actin (catalog number A2228, clone AC-74), mouse anti-human CaM (Sacks et al., 1991; catalog number 05-173), Sepharose 4B (catalog number 4B200), CaM Sepharose 4B (catalog number 17-0529-01), KN-93 (catalog number K1385), TFP (catalog number T8516), tamoxifen (catalog number T5648), and corn oil (C8267) were all purchased from Millipore Sigma. Rabbit anti-human IQGAP1 (catalog number H-109) and mouse anti-human CaMKII δ (catalog number sc-100362, clone L-04) were purchased from Santa Cruz Biotechnology. Mouse anti-HA; catalog number 2367, clone 6E2) was purchased from Cell Signaling Technology. Rabbit anti-mouse collagen IV (ab19808) and rat anti-mouse MRP14 (ab105472, clone 2B10) were purchased from Abcam. Rat anti-mouse PECAM (clone 390) was purchased from EMD Millipore. Mouse serum, goat serum, and DyLight 488- or DyLight 550-goat anti-rabbit and goat anti-mouse secondary antibodies were purchased from Jackson ImmunoResearch. Rat anti-mouse PECAM, mouse anti-human CD18, rabbit anti-mouse collagen IV, rat anti-mouse MRP14, and goat anti-Armenian hamster IgG were directly conjugated with DyLight 488, DyLight 550, or DyLight 649 (Thermo Fisher Scientific) according to the manufacturer's protocols. Goat anti-rabbit-HRP and goat anti-mouse-HRP were purchased from Bio-Rad.

Animals

All protocols and procedures involving mice were reviewed and approved by the Northwestern University Institutional Animal Care and Use Committee (Public Health Service assurance number A328301). Mice were housed in the institutional animal facility operated by the Northwestern University Center for Comparative Medicine in Chicago, IL, and were maintained according to standard Association for Assessment and Accreditation of Laboratory Animal Care protocols. All experiments in this study used mice between 8 and 12 wk of age.

The C57Bl/6 Ly6g(Cre-tdTomato) mouse strain was described previously (Hasenberg et al., 2015). Briefly, neutrophils of these mice are fluorescent because they express both Cre recombinase and the fluorescent protein tdTomato at the neutrophil-specific locus, Ly6G. To increase the fluorescence, this line was crossed with the C57Bl/6 129S6 Gt(ROSA)26Sor^{tm9(CAG-tdTomato)Hze} line (The Jackson Laboratory, catalog number 007905) to generate the *Catchup*^{IVM} mice as described (Hasenberg et al., 2015). Mice that were heterozygous for both *Ly6G*^{cre/tdTomato} and *Rosa26*^{CAG-tdTomato} were used as donors.

The C57Bl/6 GCaMP3 mouse strain was obtained from Dr. Savio Chan at Northwestern University (Evanston, IL; Cui et al., 2016). This strain contains a lox-stop-lox cassette upstream of the GCaMP3 coding region. Then, to generate mice that expressed the GCaMP3 calcium biosensor specifically in the

vascular endothelium, we crossed the GCaMP3 mice with a VE-Cadherin Cre mouse strain. The C57Bl/6 VE-Cadherin Cre mice were obtained from Dr. Gangjian Qin at Northwestern University (Evanston, IL; Zhou et al., 2013). These mice express the Cre recombinase under the VE-cadherin reporter so that its expression is limited to endothelial cells. The C57Bl/6 *Cdh5-CreERT2* mouse strain was obtained from Dr. Ralf Adams at the Max Planck Institute (Münster, Germany) and was described previously (Wang et al., 2010a).

The Black Swiss CaMKII δ ^{fl/fl} mice were obtained from J. Heller Brown at the University of California at San Diego (Ling et al., 2013). These mice were crossed with the *Cdh5-CreERT2* mouse line to generate mice in which CaMKII δ is selectively deleted in endothelial cells after induction of the Cre recombinase. To induce Cre activity, tamoxifen was dissolved in corn oil at a concentration of 20 mg/ml. 100 μ l of the tamoxifen/corn oil solution was administered via intraperitoneal injection once every 24 h for 5 d consecutively. Following the final injection, there was a 7-d waiting period before experimentation was performed. This allowed the deletion of CaMKII δ specifically in endothelial cells.

The C57Bl/6 CaMKIIN mice were obtained from I.M. Grumbach at the University of Iowa, Iowa City, IA (Murthy et al., 2017). These mice expressed a floxed eGFP sequence upstream of a stop codon that was followed by HA-tagged CaMKIIN. The CaMKIIN mice were also crossed with the *Cdh5-CreERT2* mouse strain carrying the endothelial cell-specific inducible Cre recombinase. Once Cre activity is induced with tamoxifen as described above, the floxed GFP/stop codon sequence is excised. This allows for HA-tagged CaMKIIN to be expressed specifically in endothelial cells while GFP is expressed in all nonendothelial cells that do not have Cre activity.

Bone marrow chimeras

To effectively visualize in vivo endothelial calcium signals during leukocyte TEM using intravital microscopy, bone marrow chimeras were generated using standard protocols (Duran-Struuck and Dysko, 2009; Mahajan et al., 2015). VE-Cadherin Cre GCaMP3 mice were lethally irradiated with a 1,000-cGy dose using a Gammacell 40 Exactor ¹³⁷Cs irradiator and reconstituted with bone marrow from *CatchUp*^{IVM}. Male bone marrow donors and recipients were used for imaging of the cremaster muscle. Recipients recovered for 1 mo to allow for complete bone marrow reconstitution before use in these experiments. Reconstitution was confirmed with fluorescence imaging of a blood smear (for the presence of tdTomato neutrophils).

Intravital microscopy of the mouse cremaster

The cremaster muscle from male mice was prepared for visualization using methods as previously described (Sullivan et al., 2016; Thompson et al., 2001; Woodfin et al., 2011). Male mice between 8 and 12 wk of age were intrascrotally injected with 50 ng of mouse recombinant IL-1 β (R&D Systems) and with 100 mg of DyLight 649-conjugated nonblocking rat anti-mouse PECAM (clone 390) in a final volume of 100 μ l 4 h before exteriorization and visualization of the cremaster muscle. The tissue was visualized using an Ultraview Vox imaging system

equipped with a Yokogawa CSU-1 spinning disk and a 20× water immersion objective (numerical aperture = 1.00). Images were collected using Volocity software (Perkin Elmer) and analyzed using ImageJ (National Institutes of Health; [Schneider et al., 2012](#)). Fields containing postcapillary venules with robust flow were identified using bright-field illumination. Preferred fields for imaging contained a relatively straight 30–50- μm postcapillary venule with normal, steady flow. For each field, three separate channels were acquired: green (GCaMP3 calcium signal), red (tdTomato neutrophils), and far red (anti-PECAM labeling of endothelial cell junctions). A 3D stack in the far red channel (anti-PECAM labeling of endothelial cell junctions) was first captured to determine vessel dimensions. Then a 30–60-min recording (four frames per second) of all three channels in 3D was collected to capture TEM events.

Endothelial cells and isolation of primary human peripheral blood mononuclear cells (PBMCs)

All procedures involving human subjects were approved by the institutional review board of the Northwestern University Feinberg School of Medicine. To grow endothelial cells, we used a well-established procedure to generate a stable iHUVCEC line as previously described ([Moses et al., 1999](#)). In our experience as well as in reports by several other groups, these cells grow in stable monolayers, express appropriate levels of the relevant adhesion molecules, support TEM, and overall behave identically to unmodified human umbilical vein endothelial cells (HUVECs; [Ancuta et al., 2003](#); [Watson et al., 2015](#); [Yang et al., 2005](#)). However, iHUVCECs can be transduced with adenovirus more reproducibly than HUVECs, making it preferable to use iHUVCECs for our studies.

PBMCs were isolated using standard protocols as previously described ([Muller and Luscinskas, 2008](#); [Muller and Weigl, 1992](#)). Briefly, blood was drawn from healthy volunteers into 1/10 volume EDTA (10 mM). Whole blood was then mixed with an equal volume of HBSS (Corning). The blood/HBSS mixture was layered over a Ficoll-Paque density gradient (GE Healthcare) and centrifuged at 2,200 rpm for 20 min. The upper plasma layer and the PBMC layers were collected separately. The PBMC layer was then diluted in HBSS. Both the PBMCs and plasma were centrifuged at 1,000 rpm for 10 min. The PBMC pellet was then resuspended in the spun platelet-depleted plasma and centrifuged again at 1,000 rpm for 10 min. The resultant PBMC pellet was then resuspended with HBSS and centrifuged two times at 1,000 rpm for 10 min. The final PBMC pellet was resuspended in M199 (Life Technologies) with 0.1% human serum antigen for use.

IQGAP1, CaMKIIN, dominant negative CaMKII δ constructs, and adenoviral transduction

The IQGAP1 domain truncation constructs ($\Delta 5,6$ and $\Delta 4-6$) have been generated in the laboratory and have been previously described ([Sullivan et al., 2019](#)). Briefly, we used full-length IQGAP1 in a pENTR4-GFP vector as the template to generate the IQGAP1 domain truncation constructs. The resulting constructs were then recombined with the adenoviral pAd/CMV/V5-DEST vector (Invitrogen) using LR clonase (Invitrogen). The resulting

vectors were digested with PacI and then transfected into 293A cells that produced adenovirus for transduction according to standard methods.

Adenovirus expressing HA-tagged CaMKIIN (Ad5.CMV.-CaMKIIN.HA.IRESeGFP) was generously gifted by I.M. Grumbach ([Murthy et al., 2017](#)). Adenovirus expressing HA-tagged dominant negative CaMKII δ was generously provided by J. Heller Brown ([Zhu et al., 2007, 2003](#)). The dominant negative form of CaMKII δ contains a K43A mutation. This mutation results in a catalytically dead form of the protein that prevents its kinase activity and downstream substrate phosphorylation.

For adenoviral transduction of iHUVCECs, cells were seeded on 96-well 3D collagen gels at 7,500 cells per well. The following day, monolayers were washed and incubated with fresh media overnight. On day 2 after initial seeding of cells, monolayers were washed and incubated with the indicated adenoviral construct in 100 μl of conditioned media overnight. The media were then replaced with fresh media for 24 h before the cells were used in experimentation. With this approach, the reexpression constructs were transduced for 48 h before the start of the assay.

CaM Sepharose pull-down assay

iHUVCECs were grown in 60-mm plates and were transduced with adenovirus for ~ 48 h as described above, incubated with 10 μM KN-93 30 min before experimentation, or left untreated. All experiments were done with confluent monolayers. The CaM Sepharose pull-down assay was performed as previously described ([Kaleka et al., 2012](#); [Li and Sacks, 2003](#)). Briefly, cells were washed three times with ice-cold PBS and lysed in lysis buffer composed of PBS (without Ca^{2+} or Mg^{2+}), 1% Triton X-100, 1 mM PMSF (Millipore Sigma), complete Mini protease inhibitor cocktail (Roche), and either 1 mM CaCl_2 or 1 mM EGTA. Lysates were collected and centrifuged at 14,000 rpm for 30 min at 4°C. Supernatants were recovered and precleared with Sepharose beads (Millipore Sigma; catalog number 45-165) for 1 h at 4°C with end-over-end rotation. Lysates were then incubated with CaM Sepharose beads (Millipore Sigma; catalog number 17-0529-01) on a rotator for 3 h at 4°C. Beads were then washed extensively five times with lysis buffer containing CaCl_2 or EGTA as appropriate before being resuspended in 6× Laemmli loading buffer. The samples were heated at 60°C for 30 min and processed with standard Western blotting techniques as described below.

Western blotting

Confluent iHUVCEC monolayers grown on collagen gels and transduced with adenoviral constructs as described above were washed twice with cold PBS. After washing, the cells were lysed in 50 μl PBS containing 1% NP-40, 1× protease inhibitor cocktail (Millipore Sigma; catalog number P8340), and 1 mM PMSF for 5 min at room temperature. The lysates were collected and pooled from three wells, mixed with 6× Laemmli loading buffer with β -mercaptoethanol, and heated to 60°C for 30 min. Equivalent amounts were loaded onto a 10% polyacrylamide gel and resolved using SDS-PAGE. Proteins were transferred to polyvinylidene difluoride and detected using standard Western blotting techniques. The amount of virus needed to achieve

expression levels for the constructs that were comparable to endogenous IQGAP1 or CaMKII expression levels was determined empirically for each construct.

Immunofluorescence microscopy

Confluent iHUEVCs were washed twice with PBS and fixed with 4% paraformaldehyde for 20 min at 37°C. Cells were then washed three times with PBS and permeabilized with 0.01% Triton X-100 (Millipore Sigma) for 10 min at room temperature. Blocking buffer (PBS with 5% BSA [Fraction V; Thermo Fisher Scientific] and 1% goat serum) was added for 30 min at room temperature. Cells were then incubated with primary antibody at 10 µg/ml in blocking buffer for 45 min at room temperature, washed extensively with PBS, and then incubated with secondary antibody at 4 µg/ml in blocking buffer for 45 min at room temperature protected from light. Confocal images were visualized using an Ultraview VoX imaging system equipped with a CSU-1 spinning disk. Images were acquired with a 40× oil immersion objective (numerical aperture = 1.0) using Volocity software. All images were processed and analyzed with ImageJ software.

TEM assay

TEM assays were performed as previously described on cytokine-activated endothelial cell monolayers (Muller and Lusinskas, 2008). In brief, 100 µl of the freshly isolated PBMC suspension (2×10^6 cells/ml) was added to each well of confluent iHUEVC monolayers grown on hydrated collagen gels. The PBMCs were allowed to migrate for 1 h at 37°C in 5% CO₂. The monolayers were washed two times with 1 mM EDTA in PBS (no Ca²⁺ and Mg²⁺) to disrupt lymphocyte adhesion, leaving behind monocytes. Lymphocytes do not typically adhere or migrate under these conditions; however, if any remain, they are identified based on their morphology and are not scored. Monolayers were then fixed and imaged, and monocyte transmigration was quantified according to previously described standard methods (Muller et al., 1993; Sullivan et al., 2019).

For TEM assays in which PECAM homophilic interactions were blocked, 20 µg/ml anti-PECAM (hec7) antibody was added to the leukocyte suspension for 5 min before its addition to the endothelial cell monolayers. For TEM assays in which small-molecule inhibitors were used, the endothelial cell monolayers were preincubated with either 100 µM TFP or 10 µM KN-93 in culture-conditioned media for 30 min at 37°C. The endothelial cell monolayers were then extensively washed in warm M199 before addition of the leukocytes. For TEM assays in which adenoviral constructs were transduced, the endothelial cells were transduced for ~48 h (as described above) before the addition of leukocytes for TEM.

LBRC targeted recycling assay

The targeted recycling assay to visualize the LBRC during TEM was performed as previously described (Mamdouh et al., 2009; Sullivan et al., 2019; Watson et al., 2015; Weber et al., 2015). Briefly, iHUEVC monolayers were grown to confluence on hydrated collagen gels and transduced with adenovirus ~48 h before experimentation (as described above). To perform this

assay, we first tagged total PECAM (LBRC and surface) on cytokine-activated endothelial cells with nonblocking anti-PECAM Fab IgG_{2a} fragments (clone P1.1) in culture-conditioned media. Monolayers were subsequently washed, chilled, and incubated with unlabeled F(ab')₂ secondary antibodies at 4°C to mask the surface pool of PECAM. After extensive washing of unbound antibody, PBMCs (2×10^6 cells/ml) and DyLight 550 fluorescently labeled F(ab')₂ secondary antibody were added. The leukocytes were allowed to settle on the monolayers at 4°C for 15 min, and then the samples were warmed to 37°C for 10 min to allow synchronized TEM. In this brief assay, most lymphocytes do not bind and are washed away. The few lymphocytes that do bind are easily identified morphologically and are not scored. Cells were then washed and fixed in 4% paraformaldehyde for 10 min at 4°C. Leukocytes were visualized by staining with DyLight 649-conjugated anti-CD18 after fixation.

During a brief 10-min TEM, the monocytes bind and trigger the recruitment of the LBRC. This exposes the previously unblocked primary epitopes contained within it. These epitopes are detected by the fluorescent secondary antibodies so that with confocal microscopy the recruitment of the LBRC is observed as increased fluorescence signal surrounding the migrating monocytes. For each sample, at least five fields and 20 total cells per monolayer were counted and fluorescence was quantified. Targeted recycling was considered to have occurred if the mean intensity of fluorescence around the transmigrating leukocyte was >1.5× the average intensity of the uninvolved endothelial cell border adjacent to the TEM event.

Croton oil dermatitis model and immunofluorescence staining of whole-mount ears

Croton oil-induced inflammation was performed using standard protocols as previously described (Schenkel et al., 2004; Sullivan et al., 2019). 20 µl of 0.9% croton oil in a 4:1 solution of acetone:olive oil (carrier) was applied to both leaflets of an ear for 5 h to induce inflammation. The contralateral ear was treated with carrier only. After harvesting, fixing, permeabilizing, and blocking, the ear leaflets were stained. 1 µg/ml anti-MRP14 conjugated to DyLight 488, 10 µg/ml anti-PECAM (clone 2H8) conjugated to DyLight 550, and 1 µg/ml anti-collagen IV conjugated to DyLight 649 were used for the iVE-Cre CaMKIIδ mice. 10 µg/ml anti-PECAM (clone 2H8) conjugated to DyLight 550 and 1 µg/ml anti-MRP14 conjugated to DyLight 649 were used for the iVE-Cre CaMKIIN mice.

Image processing and data collection

TEM events were defined as those where the neutrophil traversed from clearly inside of the blood vessel to clearly outside and separated from it. We centered our region of interest around the transmigratory pore as defined by PECAM labeling. Using ImageJ, we quantified the total fluorescence in this area over the entire duration of the TEM event. The GCaMP3 fluorescence images were first corrected for background by subtracting the “off vessel” value (determined using the average pixel intensity in a region of interest adjacent to the vessel). The relative fluorescence signal increase over baseline (F/F_0) around the migrating neutrophil was calculated by dividing by the average

total fluorescence in that region over the 2 min before initiation of TEM. Data are shown as a rolling average calculated by taking the mean of two consecutive frames and are graphed as a function of time. Overall, we studied a total of 12 different mice on separate days. 30 different postcapillary venule segments were studied.

For axial profile analysis, a 15- μm line was drawn centered on the pore of a TEM event, and the pixel intensity along that line was recorded for the green channel (GCaMP3 signal). The same line was then used to analyze pixel intensity for the GCaMP3 signal before the TEM event when the leukocyte was adherent to the endothelium. The individual lines from several different events were adjusted slightly to account for variations in the center of the pore. The plots were then normalized to the minimum intensity value proximal to the pore. Note that this makes the relative intensities for the plots similar at the proximal 0- μm end of the plot but retains meaningful information regarding the axial profile of the GCaMP3 signal.

Statistical analysis

All experiments were performed independently at least three times. In vitro experiments contained at least three replicates for each sample within each experiment. Average values within each experiment were averaged between experiments to produce the means and standard deviations shown here. Variance of mean values between two groups was analyzed by the Student's *t* test with a Bonferroni correction for unpaired observations. Statistical significance is denoted by asterisks, with corresponding *P* values indicated in the corresponding figure legend.

Online supplemental material

Fig. S1 demonstrates that expression of endothelial cell CaMKIIN is induced by tamoxifen. **Fig. S2** shows another mouse model in which tamoxifen induces deletion of CaMKI δ selectively in endothelial cells. **Video 1** and **Video 2** show leukocyte TEM live with intravital microscopy.

Acknowledgments

We thank Clifford D. Carpenter for assistance with experiments. We also thank Melissa Brown and Kim Broadhurst for their assistance with animal transfers. We are also grateful to Dr. Savio Chan, Dr. Gangjian Qin, and Dr. Ralf Adams for sharing their mice.

This work was supported by National Institutes of Health grants R01HL046849 and HL064774 (to W.A. Muller); National Institutes of Health grants T32GM8152 and F30HL134202, and an Alpha Omega Alpha Honor Medical Society Carolyn L. Kuckein Student Research Fellowship (to P.J. Dalal); National Institutes of Health grant R01HL108932 (to I.M. Grumbach); and National Institutes of Health grant R01HL145459 (to J. Heller Brown).

Author contributions: P.J. Dalal, D.P. Sullivan, and W.A. Muller conceived and designed this study; P.J. Dalal, D.P. Sullivan, and E.W. Weber performed the data collection and analysis; P.J. Dalal drafted the manuscript; P.J. Dalal, D.P. Sullivan, E.W. Weber, D.B. Sacks, M. Gunzer, I.M. Grumbach, J.H. Brown, and

W.A. Muller all contributed to the revision of the manuscript and approved its final version for publication.

Disclosures: I.M. Grumbach reported grants from the National Institutes of Health, the Department of Veterans Affairs, and the American Heart Association outside the submitted work. No other disclosures were reported.

Submitted: 19 December 2019

Revised: 4 May 2020

Accepted: 7 July 2020

References

- Akerboom, J., J.D. Rivera, M.M. Guilbe, E.C. Malavé, H.H. Hernandez, L. Tian, S.A. Hires, J.S. Marvin, L.L. Looger, and E.R. Schreier. 2009. Crystal structures of the GCaMP calcium sensor reveal the mechanism of fluorescence signal change and aid rational design. *J. Biol. Chem.* 284: 6455–6464. <https://doi.org/10.1074/jbc.M807657200>
- Ali, J., F. Liao, E. Martens, and W.A. Muller. 1997. Vascular endothelial cadherin (VE-cadherin): cloning and role in endothelial cell-cell adhesion. *Microcirculation.* 4:267–277. <https://doi.org/10.3109/10739689709146790>
- Ancuta, P., R. Rao, A. Moses, A. Mehle, S.K. Shaw, F.W. Lusinskas, and D. Gabuzda. 2003. Fractalkine preferentially mediates arrest and migration of CD16+ monocytes. *J. Exp. Med.* 197:1701–1707. <https://doi.org/10.1084/jem.20022156>
- Boulay, G. 2002. Ca(2+)-calmodulin regulates receptor-operated Ca(2+) entry activity of TRPC6 in HEK-293 cells. *Cell Calcium.* 32:201–207. <https://doi.org/10.1016/S0143416002001550>
- Brooks, I.M., and S.J. Tavalin. 2011. Ca2+/calmodulin-dependent protein kinase II inhibitors disrupt AKAP79-dependent PKC signaling to GluA1 AMPA receptors. *J. Biol. Chem.* 286:6697–6706. <https://doi.org/10.1074/jbc.M110.183558>
- Carman, C.V., and T.A. Springer. 2004. A transmigratory cup in leukocyte diapedesis both through individual vascular endothelial cells and between them. *J. Cell Biol.* 167:377–388. <https://doi.org/10.1083/jcb.200404129>
- Chang, B.H., S. Mukherji, and T.R. Soderling. 2001. Calcium/calmodulin-dependent protein kinase II inhibitor protein: localization of isoforms in rat brain. *Neuroscience.* 102:767–777. [https://doi.org/10.1016/S0306-4522\(00\)00520-0](https://doi.org/10.1016/S0306-4522(00)00520-0)
- Chao, L.H., M.M. Stratton, I.H. Lee, O.S. Rosenberg, J. Levitz, D.J. Mandell, T. Kortemme, J.T. Groves, H. Schulman, and J. Kuriyan. 2011. A mechanism for tunable autoinhibition in the structure of a human Ca2+/calmodulin-dependent kinase II holoenzyme. *Cell.* 146:732–745. <https://doi.org/10.1016/j.cell.2011.07.038>
- Cui, Q., J.E. Pitt, A. Pamukcu, J.F. Poulin, O.S. Mabrouk, M.P. Fiske, I.B. Fan, E.C. Augustine, K.A. Young, R.T. Kennedy, et al. 2016. Blunted mGluR Activation Disinhibits Striatopallidal Transmission in Parkinsonian Mice. *Cell Rep.* 17:2431–2444. <https://doi.org/10.1016/j.celrep.2016.10.087>
- Cyrus, B.F., and W.A. Muller. 2016. A Unique Role for Endothelial Cell Kinesin Light Chain 1, Variant 1 in Leukocyte Transendothelial Migration. *Am. J. Pathol.* 186:1375–1386. <https://doi.org/10.1016/j.ajpath.2016.01.011>
- Dalal, P.J., W.A. Muller, and D.P. Sullivan. 2020. Endothelial Cell Calcium Signaling during Barrier Function and Inflammation. *Am. J. Pathol.* 190: 535–542. <https://doi.org/10.1016/j.ajpath.2019.11.004>
- Duran-Struuck, R., and R.C. Dysko. 2009. Principles of bone marrow transplantation (BMT): providing optimal veterinary and husbandry care to irradiated mice in BMT studies. *J. Am. Assoc. Lab. Anim. Sci.* 48:11–22.
- Duza, T., and I.H. Sarelius. 2004. Localized transient increases in endothelial cell Ca2+ in arterioles in situ: implications for coordination of vascular function. *Am. J. Physiol. Heart Circ. Physiol.* 286:H2322–H2331. <https://doi.org/10.1152/ajpheart.00006.2004>
- Eriksson, J.E., T. He, A.V. Trejo-Skali, A.S. Härmälä-Braskén, J. Hellman, Y.H. Chou, and R.D. Goldman. 2004. Specific in vivo phosphorylation sites determine the assembly dynamics of vimentin intermediate filaments. *J. Cell Sci.* 117:919–932. <https://doi.org/10.1242/jcs.00906>
- Etienne-Manneville, S., J.B. Manneville, P. Adamson, B. Wilbourn, J. Greenwood, and P.O. Couraud. 2000. ICAM-1-coupled cytoskeletal rearrangements and transendothelial lymphocyte migration involve

- intracellular calcium signaling in brain endothelial cell lines. *J. Immunol.* 165:3375–3383. <https://doi.org/10.4049/jimmunol.165.6.3375>
- Frommer, W.B., M.W. Davidson, and R.E. Campbell. 2009. Genetically encoded biosensors based on engineered fluorescent proteins. *Chem. Soc. Rev.* 38:2833–2841. <https://doi.org/10.1039/b907749a>
- Giannone, G., P. Rondé, M. Gaire, J. Beaudouin, J. Haiech, J. Ellenberg, and K. Takeda. 2004. Calcium rises locally trigger focal adhesion disassembly and enhance residency of focal adhesion kinase at focal adhesions. *J. Biol. Chem.* 279:28715–28723. <https://doi.org/10.1074/jbc.M404054200>
- Guillaud, L., R. Wong, and N. Hirokawa. 2008. Disruption of KIF17-Mint1 interaction by CaMKII-dependent phosphorylation: a molecular model of kinesin-cargo release. *Nat. Cell Biol.* 10:19–29. <https://doi.org/10.1038/ncb1665>
- Hasenberg, A., M. Hasenberg, L. Männ, F. Neumann, L. Borkenstein, M. Stecher, A. Kraus, D.R. Engel, A. Klingberg, P. Seddigh, et al. 2015. Catchup: a mouse model for imaging-based tracking and modulation of neutrophil granulocytes. *Nat. Methods.* 12:445–452. <https://doi.org/10.1038/nmeth.3322>
- Hedman, A.C., J.M. Smith, and D.B. Sacks. 2015. The biology of IQGAP proteins: beyond the cytoskeleton. *EMBO Rep.* 16:427–446. <https://doi.org/10.15252/embr.201439834>
- Heemskerk, N., L. Schimmel, C. Oort, J. van Rijssel, T. Yin, B. Ma, J. van Unen, B. Pitter, S. Huvneers, J. Goedhart, et al. 2016. F-actin-rich contractile endothelial pores prevent vascular leakage during leukocyte diapedesis through local RhoA signalling. *Nat. Commun.* 7:10493. <https://doi.org/10.1038/ncomms10493>
- Ho, Y.D., J.L. Joyal, Z. Li, and D.B. Sacks. 1999. IQGAP1 integrates Ca²⁺/calmodulin and Cdc42 signaling. *J. Biol. Chem.* 274:464–470. <https://doi.org/10.1074/jbc.274.1.464>
- Huang, A.J., J.E. Manning, T.M. Bandak, M.C. Rataui, K.R. Hanser, and S.C. Silverstein. 1993. Endothelial cell cytosolic free calcium regulates neutrophil migration across monolayers of endothelial cells. *J. Cell Biol.* 120:1371–1380. <https://doi.org/10.1083/jcb.120.6.1371>
- Inagaki, N., H. Goto, M. Ogawara, Y. Nishi, S. Ando, and M. Inagaki. 1997. Spatial patterns of Ca²⁺ signals define intracellular distribution of a signaling by Ca²⁺/Calmodulin-dependent protein kinase II. *J. Biol. Chem.* 272:25195–25199. <https://doi.org/10.1074/jbc.272.40.25195>
- Jang, D.J., B. Ban, and J.A. Lee. 2011. Characterization of novel calmodulin binding domains within IQ motifs of IQGAP1. *Mol. Cells.* 32:511–518. <https://doi.org/10.1007/s10059-011-0109-4>
- Kaleka, K.S., A.N. Petersen, M.A. Florence, and N.Z. Gerges. 2012. Pull-down of calmodulin-binding proteins. *J. Vis. Exp.* (59):3502.
- Kielbassa-Schnepp, K., A. Streyl, A. Janning, L. Missiaen, B. Nilius, and V. Gerke. 2001. Endothelial intracellular Ca²⁺ release following monocyte adhesion is required for the transendothelial migration of monocytes. *Cell Calcium.* 30:29–40. <https://doi.org/10.1054/ceca.2001.0210>
- Li, Z., and D.B. Sacks. 2003. Elucidation of the interaction of calmodulin with the IQ motifs of IQGAP1. *J. Biol. Chem.* 278:4347–4352. <https://doi.org/10.1074/jbc.M208579200>
- Li, Z., S.H. Kim, J.M. Higgins, M.B. Brenner, and D.B. Sacks. 1999. IQGAP1 and calmodulin modulate E-cadherin function. *J. Biol. Chem.* 274:37885–37892. <https://doi.org/10.1074/jbc.274.53.37885>
- Liao, F., J. Ali, T. Greene, and W.A. Muller. 1997. Soluble domain 1 of platelet-endothelial cell adhesion molecule (PECAM) is sufficient to block transendothelial migration in vitro and in vivo. *J. Exp. Med.* 185:1349–1358. <https://doi.org/10.1084/jem.185.7.1349>
- Ling, H., T. Zhang, L. Pereira, C.K. Means, H. Cheng, Y. Gu, N.D. Dalton, K.L. Peterson, J. Chen, D. Bers, et al. 2009. Requirement for Ca²⁺/calmodulin-dependent kinase II in the transition from pressure overload-induced cardiac hypertrophy to heart failure in mice. *J. Clin. Invest.* 119:1230–1240. <https://doi.org/10.1172/JCI38022>
- Ling, H., C.B. Gray, A.C. Zambon, M. Grimm, Y. Gu, N. Dalton, N.H. Purcell, K. Peterson, and J.H. Brown. 2013. Ca²⁺/Calmodulin-dependent protein kinase II δ mediates myocardial ischemia/reperfusion injury through nuclear factor- κ B. *Circ. Res.* 112:935–944. <https://doi.org/10.1161/CIRCRESAHA.112.276915>
- Mahajan, M.M., B. Cheng, A.I. Beyer, U.S. Mulvaney, M.B. Wilkinson, M.E. Fomin, and M.O. Muench. 2015. A quantitative assessment of the content of hematopoietic stem cells in mouse and human endosteal-bone marrow: a simple and rapid method for the isolation of mouse central bone marrow. *BMC Hematol.* 15:9. <https://doi.org/10.1186/s12878-015-0031-7>
- Mamdouh, Z., X. Chen, L.M. Pierini, F.R. Maxfield, and W.A. Muller. 2003. Targeted recycling of PECAM from endothelial surface-connected compartments during diapedesis. *Nature.* 421:748–753. <https://doi.org/10.1038/nature01300>
- Mamdouh, Z., G.E. Kreitzer, and W.A. Muller. 2008. Leukocyte transmigration requires kinesin-mediated microtubule-dependent membrane trafficking from the lateral border recycling compartment. *J. Exp. Med.* 205:951–966. <https://doi.org/10.1084/jem.20072328>
- Mamdouh, Z., A. Mikhailov, and W.A. Muller. 2009. Transcellular migration of leukocytes is mediated by the endothelial lateral border recycling compartment. *J. Exp. Med.* 206:2795–2808. <https://doi.org/10.1084/jem.20082745>
- Moses, A.V., K.N. Fish, R. Ruhl, P.P. Smith, J.G. Strussenberg, L. Zhu, B. Chandran, and J.A. Nelson. 1999. Long-term infection and transformation of dermal microvascular endothelial cells by human herpesvirus 8. *J. Virol.* 73:6892–6902. <https://doi.org/10.1128/JVI.73.8.6892-6902.1999>
- Muller, W.A. 2011. Mechanisms of leukocyte transendothelial migration. *Annu. Rev. Pathol.* 6:323–344. <https://doi.org/10.1146/annurev-pathol-011110-130224>
- Muller, W.A. 2016a. Localized signals that regulate transendothelial migration. *Curr. Opin. Immunol.* 38:24–29. <https://doi.org/10.1016/j.coi.2015.10.006>
- Muller, W.A. 2016b. Transendothelial migration: unifying principles from the endothelial perspective. *Immunol. Rev.* 273:61–75. <https://doi.org/10.1111/imr.12443>
- Muller, W.A., and F.W. Lusinskas. 2008. Assays of transendothelial migration in vitro. *Methods Enzymol.* 443:155–176. [https://doi.org/10.1016/S0076-6879\(08\)02009-0](https://doi.org/10.1016/S0076-6879(08)02009-0)
- Muller, W.A., and S.A. Weigl. 1992. Monocyte-selective transendothelial migration: dissection of the binding and transmigration phases by an in vitro assay. *J. Exp. Med.* 176:819–828. <https://doi.org/10.1084/jem.176.3.819>
- Muller, W.A., C.M. Ratti, S.L. McDonnell, and Z.A. Cohn. 1989. A human endothelial cell-restricted, externally disposed plasmalemmal protein enriched in intercellular junctions. *J. Exp. Med.* 170:399–414. <https://doi.org/10.1084/jem.170.2.399>
- Muller, W.A., S.A. Weigl, X. Deng, and D.M. Phillips. 1993. PECAM-1 is required for transendothelial migration of leukocytes. *J. Exp. Med.* 178:449–460. <https://doi.org/10.1084/jem.178.2.449>
- Murthy, S., O.M. Koval, J.M. Ramiro Diaz, S. Kumar, D. Nuno, J.A. Scott, C. Allamargot, L.J. Zhu, K. Broadhurst, V. Santhana, et al. 2017. Endothelial CaMKII as a regulator of eNOS activity and NO-mediated vasoreactivity. *PLoS One.* 12. e0186311. <https://doi.org/10.1371/journal.pone.0186311>
- Nourshargh, S., and R. Alon. 2014. Leukocyte migration into inflamed tissues. *Immunity.* 41:694–707. <https://doi.org/10.1016/j.immuni.2014.10.008>
- Pellicena, P., and H. Schulman. 2014. CaMKII inhibitors: from research tools to therapeutic agents. *Front. Pharmacol.* 5:21. <https://doi.org/10.3389/fphar.2014.00021>
- Pfleiderer, P.J., K.K. Lu, M.T. Crow, R.S. Keller, and H.A. Singer. 2004. Modulation of vascular smooth muscle cell migration by calcium/calmodulin-dependent protein kinase II-delta 2. *Am. J. Physiol. Cell Physiol.* 286:C1238–C1245. <https://doi.org/10.1152/ajpcell.00536.2003>
- Proebstl, D., M.B. Voisin, A. Woodfin, J. Whiteford, F. D'Acquisto, G.E. Jones, D. Rowe, and S. Nourshargh. 2012. Pericytes support neutrophil sub-endothelial cell crawling and breaching of venular walls in vivo. *J. Exp. Med.* 209:1219–1234. <https://doi.org/10.1084/jem.20111622>
- Rich, R.C., and H. Schulman. 1998. Substrate-directed function of calmodulin in autophosphorylation of Ca²⁺/calmodulin-dependent protein kinase II. *J. Biol. Chem.* 273:28424–28429. <https://doi.org/10.1074/jbc.273.43.28424>
- Sacks, D.B., S.E. Porter, J.H. Ladenson, and J.M. McDonald. 1991. Monoclonal antibody to calmodulin: development, characterization, and comparison with polyclonal anti-calmodulin antibodies. *Anal. Biochem.* 194:369–377. [https://doi.org/10.1016/0003-2697\(91\)90243-M](https://doi.org/10.1016/0003-2697(91)90243-M)
- Schenkel, A.R., Z. Mamdouh, X. Chen, R.M. Liebman, and W.A. Muller. 2002. CD99 plays a major role in the migration of monocytes through endothelial junctions. *Nat. Immunol.* 3:143–150. <https://doi.org/10.1038/nr1749>
- Schenkel, A.R., T.W. Chew, and W.A. Muller. 2004. Platelet endothelial cell adhesion molecule deficiency or blockade significantly reduces leukocyte emigration in a majority of mouse strains. *J. Immunol.* 173:6403–6408. <https://doi.org/10.4049/jimmunol.173.10.6403>
- Schneider, C.A., W.S. Rasband, and K.W. Eliceiri. 2012. NIH Image to ImageJ: 25 years of image analysis. *Nat. Methods.* 9:671–675. <https://doi.org/10.1038/nmeth.2089>
- Song, J., X. Zhang, K. Buscher, Y. Wang, H. Wang, J. Di Russo, L. Li, S. Lütken-Enking, A. Zarbock, A. Stadtmann, et al. 2017. Endothelial Basement

- Membrane Laminin 511 Contributes to Endothelial Junctional Tightness and Thereby Inhibits Leukocyte Transmigration. *Cell Rep.* 18:1256–1269. <https://doi.org/10.1016/j.celrep.2016.12.092>
- Su, W.H., H.I. Chen, J.P. Huang, and C.J. Jen. 2000. Endothelial [Ca(2+)](i) signaling during transmigration of polymorphonuclear leukocytes. *Blood.* 96:3816–3822. <https://doi.org/10.1182/blood.V96.12.3816>
- Suetomi, T., A. Willeford, C.S. Brand, Y. Cho, R.S. Ross, S. Miyamoto, and J.H. Brown. 2018. Inflammation and NLRP3 Inflammasome Activation Initiated in Response to Pressure Overload by Ca²⁺/Calmodulin-Dependent Protein Kinase II δ Signaling in Cardiomyocytes Are Essential for Adverse Cardiac Remodeling. *Circulation.* 138:2530–2544. <https://doi.org/10.1161/CIRCULATIONAHA.118.034621>
- Sullivan, D.P., M.A. Seidman, and W.A. Muller. 2013. Poliovirus receptor (CD155) regulates a step in transendothelial migration between PECAM and CD99. *Am. J. Pathol.* 182:1031–1042. <https://doi.org/10.1016/j.ajpath.2012.11.037>
- Sullivan, D.P., C. Ruffer, and W.A. Muller. 2014. Isolation of the lateral border recycling compartment using a diaminobenzidine-induced density shift. *Traffic.* 15:1016–1029. <https://doi.org/10.1111/tra.12184>
- Sullivan, D.P., R.L. Watson, and W.A. Muller. 2016. 4D intravital microscopy uncovers critical strain differences for the roles of PECAM and CD99 in leukocyte diapedesis. *Am. J. Physiol. Heart Circ. Physiol.* 311:H621–H632. <https://doi.org/10.1152/ajpheart.00289.2016>
- Sullivan, D.P., P.J. Dalal, F. Jaulin, D.B. Sacks, G. Kreitzer, and W.A. Muller. 2019. Endothelial IQGAP1 regulates leukocyte transmigration by directing the LBRC to the site of diapedesis. *J. Exp. Med.* 216:2582–2601. <https://doi.org/10.1084/jem.20190008>
- Tang, J., Y. Lin, Z. Zhang, S. Tikunova, L. Birnbaumer, and M.X. Zhu. 2001. Identification of common binding sites for calmodulin and inositol 1,4,5-trisphosphate receptors on the carboxyl termini of trp channels. *J. Biol. Chem.* 276:21303–21310. <https://doi.org/10.1074/jbc.M102316200>
- Thompson, R.D., K.E. Noble, K.Y. Larbi, A. Dewar, G.S. Duncan, T.W. Mak, and S. Nourshargh. 2001. Platelet-endothelial cell adhesion molecule-1 (PECAM-1)-deficient mice demonstrate a transient and cytokine-specific role for PECAM-1 in leukocyte migration through the perivascular basement membrane. *Blood.* 97:1854–1860. <https://doi.org/10.1182/blood.V97.6.1854>
- Tian, L., S.A. Hires, T. Mao, D. Huber, M.E. Chiappe, S.H. Chalasani, L. Petreanu, J. Akerboom, S.A. McKinney, E.R. Schreiter, et al. 2009. Imaging neural activity in worms, flies and mice with improved GCaMP calcium indicators. *Nat. Methods.* 6:875–881. <https://doi.org/10.1038/nmeth.1398>
- Vandonselaar, M., R.A. Hickie, J.W. Quail, and L.T. Delbaere. 1994. Trifluoperazine-induced conformational change in Ca(2+)-calmodulin. *Nat. Struct. Biol.* 1:795–801. <https://doi.org/10.1038/nsb1194-795>
- Wang, Y., M. Nakayama, M.E. Pitulescu, T.S. Schmidt, M.L. Bochenek, A. Sakakibara, S. Adams, A. Davy, U. Deutsch, U. Lüthi, et al. 2010a. Ephrin-B2 controls VEGF-induced angiogenesis and lymphangiogenesis. *Nature.* 465:483–486. <https://doi.org/10.1038/nature09002>
- Wang, Z., R. Ginnan, I.F. Abdullaev, M. Trebak, P.A. Vincent, and H.A. Singer. 2010b. Calcium/Calmodulin-dependent protein kinase II delta 6 (CaMKII δ 6) and RhoA involvement in thrombin-induced endothelial barrier dysfunction. *J. Biol. Chem.* 285:21303–21312. <https://doi.org/10.1074/jbc.M110.120790>
- Watson, R.L., J. Buck, L.R. Levin, R.C. Winger, J. Wang, H. Arase, and W.A. Muller. 2015. Endothelial CD99 signals through soluble adenylyl cyclase and PKA to regulate leukocyte transendothelial migration. *J. Exp. Med.* 212:1021–1041. <https://doi.org/10.1084/jem.20150354>
- Weber, E.W., F. Han, M. Tauseef, L. Birnbaumer, D. Mehta, and W.A. Muller. 2015. TRPC6 is the endothelial calcium channel that regulates leukocyte transendothelial migration during the inflammatory response. *J. Exp. Med.* 212:1883–1899. <https://doi.org/10.1084/jem.20150353>
- Willeford, A., T. Suetomi, A. Nickle, H.M. Hoffman, S. Miyamoto, and J. Heller Brown. 2018. CaMKII δ -mediated inflammatory gene expression and inflammasome activation in cardiomyocytes initiate inflammation and induce fibrosis. *JCI Insight.* 3. e97054. <https://doi.org/10.1172/jci.insight.97054>
- Wong, M.H., A.B. Samal, M. Lee, J. Vlach, N. Novikov, A. Niedziela-Majka, J.Y. Feng, D.O. Koltun, K.M. Brendza, H.J. Kwon, et al. 2019. The KN-93 Molecule Inhibits Calcium/Calmodulin-Dependent Protein Kinase II (CaMKII) Activity by Binding to Ca²⁺/CaM. *J. Mol. Biol.* 431:1440–1459. <https://doi.org/10.1016/j.jmb.2019.02.001>
- Woodfin, A., M.B. Voisin, M. Beyrau, B. Colom, D. Caille, F.M. Diapouli, G.B. Nash, T. Chavakis, S.M. Albelda, G.E. Rainger, et al. 2011. The junctional adhesion molecule JAM-C regulates polarized transendothelial migration of neutrophils in vivo. *Nat. Immunol.* 12:761–769. <https://doi.org/10.1038/ni.2062>
- Wright, S.D., P.E. Rao, W.C. Van Voorhis, L.S. Craigmyle, K. Iida, M.A. Talle, E.F. Westberg, G. Goldstein, and S.C. Silverstein. 1983. Identification of the C3bi receptor of human monocytes and macrophages by using monoclonal antibodies. *Proc. Natl. Acad. Sci. USA.* 80:5699–5703. <https://doi.org/10.1073/pnas.80.18.5699>
- Yang, L., R.M. Froio, T.E. Sciuto, A.M. Dvorak, R. Alon, and F.W. Lusinskas. 2005. ICAM-1 regulates neutrophil adhesion and transcellular migration of TNF-alpha-activated vascular endothelium under flow. *Blood.* 106:584–592. <https://doi.org/10.1182/blood-2004-12-4942>
- Zhang, Z., J. Tang, S. Tikunova, J.D. Johnson, Z. Chen, N. Qin, A. Dietrich, E. Stefani, L. Birnbaumer, and M.X. Zhu. 2001. Activation of Trp3 by inositol 1,4,5-trisphosphate receptors through displacement of inhibitory calmodulin from a common binding domain. *Proc. Natl. Acad. Sci. USA.* 98:3168–3173. <https://doi.org/10.1073/pnas.051632698>
- Zhou, J., M. Wu, S. Xu, M. Cheng, C. Ding, Y. Liu, H. Yan, D. Biyashev, R. Kishore, and G. Qin. 2013. Contrasting roles of E2F2 and E2F3 in cardiac neovascularization. *PLoS One.* 8. e65755. <https://doi.org/10.1371/journal.pone.0065755>
- Zhu, W.Z., S.Q. Wang, K. Chakir, D. Yang, T. Zhang, J.H. Brown, E. Devic, B.K. Kobilka, H. Cheng, and R.P. Xiao. 2003. Linkage of beta1-adrenergic stimulation to apoptotic heart cell death through protein kinase A-independent activation of Ca²⁺/calmodulin kinase II. *J. Clin. Invest.* 111:617–625. <https://doi.org/10.1172/JCI200316326>
- Zhu, W., A.Y. Woo, D. Yang, H. Cheng, M.T. Crow, and R.P. Xiao. 2007. Activation of CaMKII δ is a common intermediate of diverse death stimuli-induced heart muscle cell apoptosis. *J. Biol. Chem.* 282:10833–10839. <https://doi.org/10.1074/jbc.M611507200>

Supplemental material

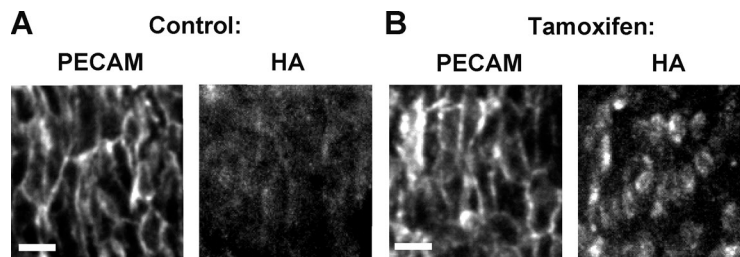


Figure S1. **Tamoxifen induces endothelial cell CaMKIIN expression in vivo.** The inducible VE-Cadherin CaMKIIN mice expressed a floxed eGFP sequence upstream of a stop codon followed by an HA-tagged CaMKII inhibitor peptide, CaMKIIN (HA-tagged CaMKIIN). Once Cre recombinase activity was induced with tamoxifen, the floxed GFP/stop codon sequence was excised, allowing expression of CaMKIIN selectively in endothelial cells. **(A)** Immunofluorescence of whole mount of the control aorta shows absence of HA-tagged CaMKIIN staining in control endothelial cells. **(B)** Immunofluorescence of whole mount of the aorta of mice injected with tamoxifen shows that expression of HA-tagged CaMKIIN is indeed specifically induced in endothelial cells. Furthermore, CaMKIIN expression does not have any effect on endothelial cell morphology or PECAM expression. At least three fields from three independent experiments were evaluated, and representative images are shown. Scale bar is 10 μ m.

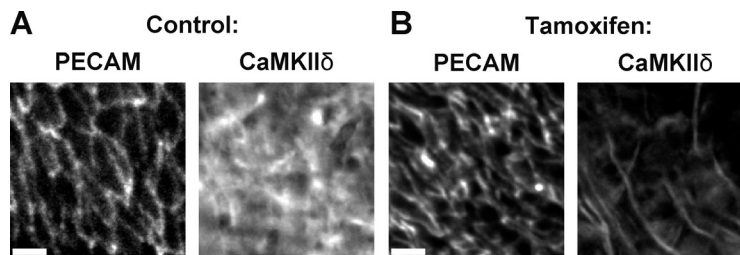


Figure S2. **Tamoxifen induces deletion of CaMKII δ in endothelial cells in vivo.** The inducible VE-Cadherin CaMKII $\delta^{fl/fl}$ mice exhibit selective deletion of CaMKII δ in endothelial cells after induction of the Cre recombinase with tamoxifen. **(A)** Immunofluorescence of the whole mount of the control aorta demonstrates CaMKII δ expression in endothelial cells. **(B)** Immunofluorescence of whole mount of the aorta after tamoxifen injections shows that expression of CaMKII δ is specifically deleted in endothelial cells. Residual staining that appears as streaks in the tamoxifen-treated, CaMKII δ -stained sample is an artifact created by folds during the tissue mounting process and not residual expression. Furthermore, deletion of CaMKII δ does not have any effect on endothelial cell morphology or PECAM expression. At least three fields from three independent experiments were evaluated, and representative images are shown. Scale bar is 10 μ m.

Video 1. **Leukocyte TEM is shown live with intravital microscopy.** Here, the endothelial calcium signal is fluorescent in the green channel, transmigrating neutrophils are fluorescent in the red channel, and endothelial cells are outlined in the far red channel. Arrows highlight neutrophil transmigration events and the corresponding endothelial calcium signal. This video was acquired at 1 frame/9 s, and the playback frame rate is 7 frames/s.

Video 2. **Leukocyte TEM is also shown with intravital microscopy.** Here, the endothelial calcium signal is fluorescent in the green channel, neutrophils are labeled using an anti-CD18 antibody and are fluorescent in the far red channel, and endothelial cells are outlined in the red channel. The arrow highlights a neutrophil transmigration event and the corresponding endothelial calcium signal. This video was acquired at 3 frames/min, and the playback frame rate is 4 frames/s.